ORCHESTRATING INTER-DATACENTER BULK TRANSFERS WITH CODEDBULK

A Dissertation

Presented to the Faculty of the Graduate School

of Cornell University

in Partial Fulfillment of the Requirements for the Degree of

Doctor of Philosophy

by

Shih-Hao Tseng

December 2018

ORCHESTRATING INTER-DATACENTER BULK TRANSFERS WITH CODEDBULK

Shih-Hao Tseng, Ph.D.

Cornell University 2018

Over the past decades, data centers are built across the globe in response to the ever-growing Internet traffic. The data centers are managed and operated by the service providers through private inter-datacenter wide area networks (WANs). Unlike WANs involving multiple service providers, these private inter-datacenter WANs exhibit a number of unique characteristics. For example, the end-hosts and the network fabric are controlled by one single provider; scheduled bulk traffic transfers terabits of data across expensive WAN links for replication and migration; also, major service providers embrace software-defined networking (SDN) in their inter-datacenter WANs for easier management and better performance. These unique characteristics enable new solutions that were either infeasible or impractical in traditional WANs.

We present CodedBulk, an end-to-end system that reduces the bandwidth required for inter-datacenter bulk transfers. CodedBulk is rooted in a known technique from the information theory community – network coding. Network coding has been known not only for its significant theoretical benefits but also for its challenging real-world implementation and adoption. CodedBulk addresses the technical implementation challenges of network coding by exploiting the unique characteristics of inter-datacenter bulk transfers. The design of CodedBulk is agnostic to the underlying transport layer, which allows smooth integration into existing infrastructure. We run our system prototype

on inter-datacenter networks, and it demonstrates a significant throughput improvement resulting from the bandwidth reduction.

BIOGRAPHICAL SKETCH

Shih-Hao Tseng earned his Bachelor of Science degree in Engineering, with a minor in Economics, from National Taiwan University, Taiwan, in 2012. He graduated as an Honorary Member of the Phi Tau Phi Scholastic Honor Society.

Later, he joined the M.S/Ph.D program in the School of Electrical and Computer Engineering at Cornell University in August, 2013. Since then, he worked as a member of the Networks Group led by Dr. A. Kevin Tang, focusing on the fundamental limits and efficient algorithm designs in the era of software-defined networking and network function virtualization. While pursuing his degree, he also interned at AT&T in 2016 and cooperated with Dr. John C.S. Lui as a research assistant at the Chinese University of Hong Kong in 2017.

He was a recipient of the Studying Abroad Scholarship from Taiwan's Ministry of Education, the Jacobs Fellowship, and the George W. Holbrook Jr. '52 Graduate Research Award. His research interests include networks, control, and optimization.

This dissertation is dedicated to my wife Ling, my parents, and my whole family for their unconditional support and love during the challenges of graduate school and life.

ACKNOWLEDGEMENTS

Throughout the fruitful five years at Cornell, the one I would like to thank the most should be my adviser professor A. Kevin Tang. Kevin has always been a supportive mentor who not only guides me through the process toward an independent researcher but also grants me much freedom to explore my research interests. Besides the techniques I learned from him, I especially cherish the vision and the philosophy of doing research that he shared with me. Meanwhile, I also want to thank my committee for their advice and guidance. Professor Lang Tong taught me how to present in an academic way right after I started my PhD. I enjoyed collaborating with professor Eilyan Y. Bitar on several interesting control projects. He also emphasized to me the importance of fluent oral presentation, which I then kept on practicing in the following years.

In addition to my committee, I want to thank several professors for their inspiring courses (sorted by the last name): Rachit Agarwal, Hsiao-Dong Chiang, David F. Delchamps, Adrian Lewis, Emin Gun Sirer, Aaron B. Wagner, and David P. Williamson. Especially, the "law of conservation of writing and reading effort" by professor Wagner has a significant impact on my writing. The administrative staff at Cornell is superb. Scott E. Coldren, T. Daniel Richter, and Patricia L. Gonyea helped me a lot during my PhD years.

I have met several amazing people at Cornell. It is my pleasure to work with the members of Cornell Networks Group: Nithin Michael, Chiun Lin Lim, Andrey Gushchin, Ning Wu, Yingjie Bi, and Jiangnan Cheng. My office mates that share Rhodes 359 with me – Yiting Xie, Shuang Liu, Evan Yu, and Zhilu Zhang – broaden my horizons. I would miss the Friday jogging with the people of the Fried Chicken Running Club: Rohit R Singh, Yi (James) Xia, and Matsuoka Fumiaki (including the founders Chun-Ti Chang and Hung-Lun Hsu, who will be

mentioned later). I also cherish the friendships since the first-year TA training class: Kittikun Chris Songsomboon, Suwon Bae, Misook Park, and Zhen Tan.

These five years, my ECE (and MAE) friends have been pretty supportive: Charles Jeon, Ramina Ghods, Oscar Castañeda, Florian Glaser, Khalid Al-Hawaj, Ritchie Zhao, Raphael Louca, Weixuan Lin, Kia Khezeli, Ibrahim Issa, Nirmal Shende, Omer Bilgen, Sevi Baltaoğlu, Earth Visarute Pinrod, Robert Owusu-Mireku, and Kevin J. Kircher. I still remember the day when Charles greeted with me in the orientation. Since then, he has been my good friend and given me good advice at several critical moments throughout my PhD.

I am also grateful for the support from my Taiwanese friends Hung-Lun Hsu, Wei-Liang Chen, Ju-Chen Chia, Kevin Lee, Yi-Hsiang (Sean) Lai, Han-Yuan Liu, Jen-Yu Huang, Chih-Chieh (Tracy) Huang, Kai-Yuan Chen, Chun-Ti Chang, Michelle Lee, and Hong Kong friend Henry Chu. They helped me deal with several difficulties I encounter in a foreign environment. Hung-Lun has been a great housemate who shared with me a lot of information about starting a new life here.

Thanks also to other Taiwanese (and Hong Kong) people in Ithaca: Wei-Hua Chang, Wen-Hsuan Chang, Chih-Yin Chen, I-Tzu (Wanda) Chen, Jiun-Reuy Chen, Po-Cheng Chen, Ting-Hsuan (Julia) Chen, Wei-Han (Brian) Chen, Yi-Chen (Eric) Chiang, Ying-Ling Chiang, Joyce Fang, Yi-Yun Ho, Hsien-Lien Huang, Ding-Yuan Kuo, Wei-Chih Kuo, Ti-Yen Lan, Ben Li, Jui-Yun Liao, Kuan-Chuan Peng, Hsiang-Han Su, Lieh-Ting (Adrian) Tung, Dah-Jiun Fu, Yi-An Yang, and Yu-Chern (Chad) Wong. The life here would be so dull without the memories and the activities we had together.

My family deserves a special place on this list. I thank my father Chun-Sheng Tseng, my mother Shu-Yi Yen, and my sister Yu-Fen Tseng. Without their

unconditional love, support, and encouragement, I would have never pursued my PhD thousand miles away from Taiwan five years ago.

Above all, my deepest gratitude goes to my wife, Ling. Her constant support and love are critical for me to overcome the obstacles along the way down the academic path. Thank you for accompanying me through the dark and the bright, day and night, sunset and sunrise.

TABLE OF CONTENTS

LIST OF TABLES

LIST OF FIGURES

CHAPTER 1

INTRODUCTION

1.1 Motivation

Today, web and cloud-based applications like search engines, social networks, online file storage, video streaming, etc., provide services to potentially millions of users and therefore the service providers require dedicated data centers to store and process the large amounts of application and user data [1, 2, 3]. Moreover, these providers often use multiple of such data centers spread geographically in order to provide improved user-level performance and fault-tolerance [4, 5]. These data centers are connected via private WANs, with links which can span across continents [6, 7]. Further, these links carry traffic at rates above several terabits per second, resulting in very high associated infrastructure costs [7]. Moreover, additional objectives for the providers, like guaranteeing at least over five nines of reliability [8], requires the operators to overprovision the network, achieving less than half of the WAN utilization on average [6, 7], adding further to the cost of the inter-datacenter networks.

Several designs [6, 7] tried to curb this under-utilization by employing centralized traffic engineering to dynamically adapt the rates at which traffic is sent across the inter-datacenter network, particularly the delay-tolerant bulk-traffic or the background traffic, which forms the majority of the data sent across the inter-datacenter network [7, 9, 10]. Contrary to the low-volume, higher-priority interactive traffic, bulk-traffic does not directly impact user-level performance thus does not have any application specific deadlines [7]. One of the main sources of bulk traffic is data replication – providers create geographically iso-

lated copies of data for higher fault-tolerance and resilience, cache highly accessed data near to the locations with higher demands for reduced latency, or simply create multiple backup copies for scheduled maintenance. Since a large fraction of inter-datacenter traffic is bulk traffic, our main goal would be to reduce the required amount of bandwidth for the bulk-traffic, which accounts for the major chunk of the infrastructure costs of the inter-datacenter networks.

The continuing decrease of the price and the power consumption of computation and storage at data centers leads to new design opportunities: We can use computation and storage sources in exchange for lower bandwidth utilization – through network coding. By treating the data as bits rather than commodities, network coding, a subfield in information theory, illustrates that an appropriate coding scheme allows each destination in a multicast session to reach its max-flow throughput without additional link capacity [11, 12]. In other words, network coding has the potential to send more data using less bandwidth.

1.2 Related Work

inter-datacenter Networks inter-datacenter networks interconnect geographically distributed data centers. Two well-known examples are SDN-enabled Google's B4 [6] and Microsoft's SWAN [7]. Managing the wide-spread data across inter-connected data centers is a challenging task, and a large fraction of the literature addresses this issue. Microsoft's Volley automatically places application data across geo-distributed data centers while taking into account the data sharing and inter-dependency [13]. Google operates a global scale database named Spanner [14]. Mesa, a data warehousing system, handles the

measurement data related to Google's advertising business across multiple data centers [15]. SPANStore provides a unified view of the storage services across geo-distributed data centers [16]. JetStream aggregates and degrades the stored data to save the bandwidth needed to assemble the data [17]. Iridium aims to achieve low latency geo-distributed analytics by prelocating datasets before the arrivals of the queries [18]. Geode saves the inter-datacenter bandwidth for performing data analytics by caching the intermediate results and transferring only the differences [19].

Routing and Scheduling on inter-datacenter Networks The significant expense of network capacity leads to the scarcity of wide-area bandwidth [13, 19]. Therefore, inter-datacenter operators aim to achieve high utilization of their expensive links [6, 7]. NetStitcher leverages the in-network storage to store and schedule the bulk traffic to fully utilize the network bandwidth [10]. [20] transfers delay-tolerant bulk data through the Internet using off-peak prepaid bandwidth via source scheduling policies.

Meanwhile, the growing inter-datacenter traffic imposes higher requirements on routing and scheduling. Owan controls both the optical devices and the network layer to route bulk traffic through wide-area network [21]. [4] proposes routing algorithms to steer bulk traffic through an inter-datacenter network by an SDN controller. TEMPUS performs online temporal planning to meet the deadline for both short-term and long-term demands [22]. Amoeba also schedules inter-datacenter traffic to meet the deadline using admission control [23].

Multicast Point to multiple points transfer is one of the long-lasting topics in networking. Classical multicast solutions focus on the construction of and the load balancing among a forest of multicast trees [24, 25, 26, 27, 28]. There is also a line of work focusing on application layer multicasting such as [29], and we refer the reader to [30] for a comprehensive survey.

Network Coding With negligible link latency, network coding demonstrates that min-cut throughput can be achieved per destination by coding the symbols [11]. [12] then shows that linear codes are sufficient for achieving the min-cut throughput. As to how the linear codes can be generated, [31] proposes algebraic network coding that takes into account the information sent to each destination; [32] uses random network coding that codes the symbols randomly while maintaining probabilistic decoding guarantees; [33] gives a polynomial time algorithm to compute the linear codes for each edge in a topological-ordered network. In our work, we generalize the method in [33] to deal with any given path sets.

A few attempts were made in the past to build a system that employs network coding to improve throughput. One of the proposals is [34], which incorporates the encoding vectors into the packets and the packets are distinguished by different redundancy offsets. Another design is COPE [35]. COPE aims to perform network coding under wireless environments. One key difference between a wireless and a wired network is that the packets are broadcast to all neighboring nodes in a wireless network, while the packet flows are routed through paths in a wired network. As a result, COPE focuses on per-hop coding benefit rather than end-to-end coding as considered in this work. For radio networks, analog network coding (ANC) proposes to exploit the interference,

which is essentially a summation operation of the signals, to increase the network capacity [36].

Although the above designs focus on practical networks, their deployment to real networks is rarely seen as those designs run on routers [34] or base stations [35, 36], which require the upgrade of the current devices to support computationally-intense network coding functionality.

Other Network Coded Systems Network coding is also considered useful for other purposes [37]. A line of work focuses on coding different segments or blocks in the TCP connection to improve the robustness [38, 39]. [40] simulates the benefit of network coding for a large-scale content distribution system. A distributed storage system can also adopt network coding to reduce the stored data while providing the same level of reliability [41]. The reader is referred to [42] for a comprehensive survey.

1.3 Contributions and Organization of the Dissertation

We present CodedBulk, the first inter-datacenter bulk transfer system that employs network coding to reduce the bandwidth utilization of the bulk traffic. CodedBulk demonstrates a 2× to 4× throughput improvement of the bulk traffic over the non-coded cases without disturbing the interactive counterpart in geo-distributed wide-area networks. The benefits are offered by overcoming the following challenges.

Multiple coded multicast sessions In an inter-datacenter network, multiple multicast sessions can exist for data replication among different data centers. Network coding saves the occupied bandwidth of each multicast session while allocating bandwidth to multiple coded multicast flows involves fairness and performance concerns, which remains open nowadays. By performing coding at the application layer, load balancing among multiple coded multicast sessions is achieved automatically by TCP fair sharing on each link.

Interactive non-coded traffic inter-datacenter networks have both the bulk and the interactive traffic. The time-sensitive non-coded interactive traffic is usually assigned a higher priority, which would make bulk traffic lack available bandwidth. Such shared network condition is not considered in the traditional network coding papers, which focus on a network dedicated to one coded traffic only. CodedBulk addresses the bandwidth imbalance issues caused by the interactive traffic by a bi-priority design that allows the coded bulk traffic to adapt to bandwidth imbalance and utilize the available bandwidth fully.

Asymmetric delay and network asynchrony The latency varies among different pairs of data centers in an inter-datacenter network due to the geographical distance and the underlying queueing policies. The asymmetric delay pattern results in network asynchrony that prevents the nodes to collect all the required coding inputs at the same time, which serves as a foundation in most of the network coding literature. To deal with network asynchrony, we introduce the store-and-forward model using multihop TCPs. Unlike the end-to-end TCP which performs rate control over one path. Multihop TCPs require some flow control scheme to handle several segments. We apply a simple backpressure

mechanism to ensure the multihop TCPs converge to the bottleneck capacity.

The dissertation is organized as follows. We first provide the network coding preliminaries in Chapter 2. An overview of CodedBulk is given in Chapter 3 to discuss the opportunities, challenges, design decisions, and system architecture. The detailed architecture descriptions are elaborated in Chapter 4, followed by our proposed coding algorithm in Chapter 5. We illustrate in Chapter 6 the implementation challenges and our solutions. The performance of the implemented CodedBulk is evaluated in Chapter 7. Chapter 8 summarizes the design and lists some possible future directions.

CHAPTER 2

NETWORK CODING PRILIMINARIES

2.1 Benefits of Network Coding: the Butterfly Example

Network coding is a subfield in information theory that examines the maximum achievable throughput from a source to each of the destinations. One of the first network coding examples demonstrated in [11] is the *butterfly example* as shown in Figure 2.1.

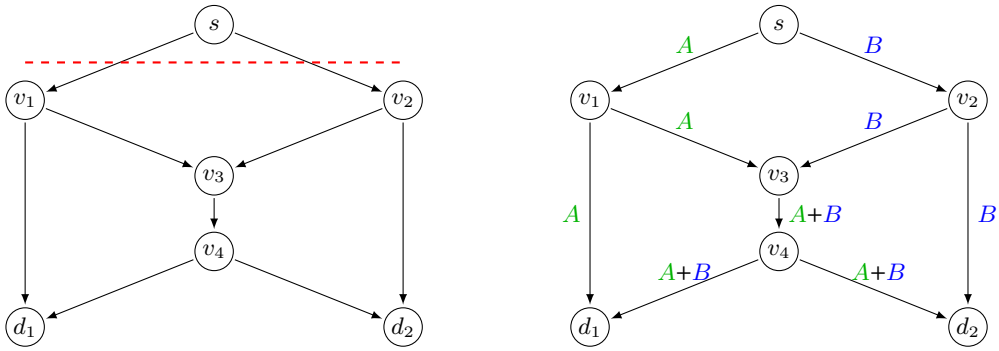

(a) The network topology and the min-cut of capacity 2.

(b) Network coding enables each destination to achieve throughput 2.

Figure 2.1: The butterfly example. The source s multicasts to two destinations d_1 and d_2 on a directed unit-capacity network.

The butterfly example is established on a directed network consisting of unit capacity links, with one source s multicasting to two destinations d_1 and d_2. Disregarding transmission and processing delays – the delays of going through a link and a node – and treating the disseminated data as commodities, the maximum aggregate throughput received at all of the destinations is bounded by the min-cut capacity of the network topology, which is 2 as shown by the dashed red line in Figure 2.1(a).

An important observation made by [11] is that the disseminated information can not only be relayed as commodities but also be coded and decoded as bits. Figure 2.1(b) shows one possible *coding scheme*, a set of codes for a multicast flow, that improves the aggregate throughput. Let A and B be two bits sent out from s at the same time. The node v_3 combines A and B by a modulo 2 addition (written as +), or an exclusive-or (XOR) operation. By doing so, both destinations d_1 and d_2 have sufficient information to decode A and B independently. As a result, the throughput per destination is 2, and the aggregate throughput is boosted to 4, which is twice the throughput without coding.

2.2 Max-Flow/Min-Cut Theorems

The butterfly example reveals that the multicast throughput can be improved through coding, and a natural followup question is how much gain can be obtained by appropriate designed coding schemes. The question is answered by the Theorem 1 in [11], which we summarize in the following theorems.

Theorem 2.2.1 (Max-Flow Theorem)**.** *There exists a coding scheme that achieves the max-flow throughput of a (multicast) flow from the source to each destination.*

Since the well-known *max-flow min-cut theorem* suggests that the max-flow equals to the min-cut, we can express Theorem 2.2.1 in its dual form as follows.

Theorem 2.2.2 (Min-Cut Theorem)**.** *There exists a coding scheme that achieves the min-cut capacity of a (multicast) flow from the source to each destination.*

The butterfly example is a case achieving the min-cut capacity. As in Figure 2.1(a), the min-cut from s to either d_1 or d_2 is 2, and the codes allows both d_1

and d_2 to reach their min-cut capacities.

2.3 Linear Network Coding

Although Theorem 2.2.1 (and Theorem 2.2.2) depicts the maximum achievable throughput, it does not dictate which coding schemes should be used. In general, there exist multiple coding schemes that all achieve per destination max-flow.

As an illustration, we revisit the butterfly example in Figure 2.2. Figure 2.2(a) shows a coding scheme, different from the one in Figure 2.1(b), which also allows both destinations to decode A and B. It is possible to design an even more complicated coding scheme to send max-flow to each destination like the one in Figure 2.2(b), which involves negations.

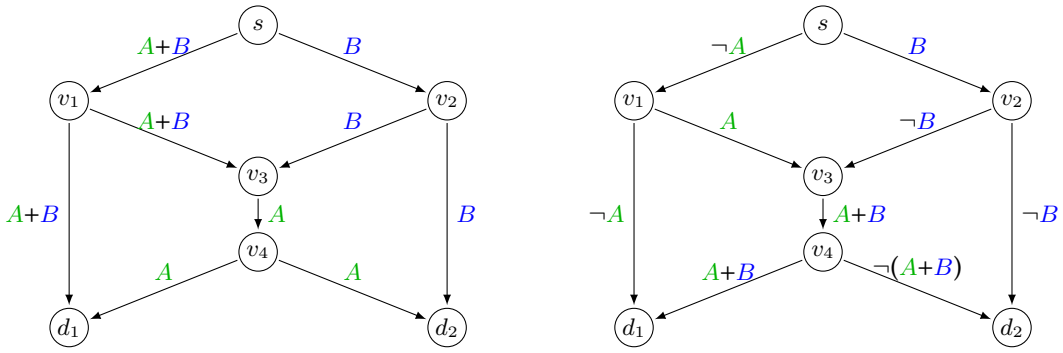

(a) Another coding scheme that leads to per destination max-flow.

(b) A more complicated coding scheme involving negation (¬).

Figure 2.2: Multiple coding schemes exist to achieve the min-cut capacity.

Despite the existence of numerous coding schemes, it is critical to ask how *one* coding scheme can be obtained. [12] suggests one focus on *linear codes* only. We illustrate what linear codes are as follows.

2.3.1 Symbols, Base Fields, and Information Vectors

Instead of referring to the disseminated data in bits, we deem them as *symbols* over some *base field* in the sense of information theory. Each symbol represents a fixed length series of bits, and the size of the corresponding base field is the number of distinct symbols. For instance, a symbol representing 1 bit belongs to a base field of size $2^1 = 2$. Similarly, an 8-bit symbol indicates a base field of size $2^8 = 256$.

The information transmitted from the source is partitioned into fixed dimension row vectors of symbols. Such row vectors are named *information vectors*. In the butterfly example, each information vector, previously written by $\begin{bmatrix} A & B \end{bmatrix}$, has dimension 2.

Given an information vector, the linear codes specify the linear combinations of the symbols in the information vector in the form of column vectors. Figure 2.3 shows the column vectors that lead to the same coding scheme as the one in Figure 2.1(b).

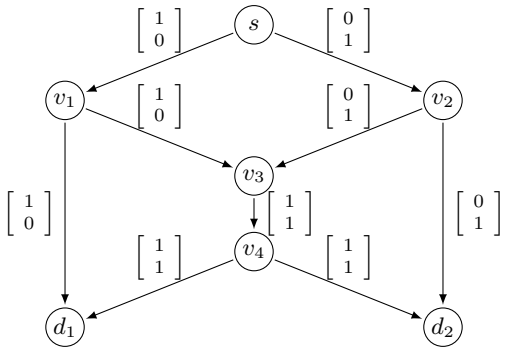

Figure 2.3: Linear coding expresses each coded symbol by a column vector.

The inner product of the information vector and the column vector gives

the corresponding sent symbol. For instance, symbol A is sent through (s, v_1) in Figure 2.1(b), which can be written as

$$A = 1 \cdot A + 0 \cdot B = \begin{bmatrix} A & B \end{bmatrix} \begin{bmatrix} 1 \\ 0 \end{bmatrix}.$$

Therefore, the column vector $\begin{bmatrix} 1 \\ 0 \end{bmatrix}$ gives symbol A. Similarly, the symbol $A + B$ can be represented by the column vector $\begin{bmatrix} 1 \\ 1 \end{bmatrix}$ as it can be written as

$$A + B = 1 \cdot A + 1 \cdot B = \begin{bmatrix} A & B \end{bmatrix} \begin{bmatrix} 1 \\ 1 \end{bmatrix}.$$

2.3.2 Generalization to Finite Fields

Besides the binary base field in the above example, linear coding can also be generalized for a field with a larger base field size by adopting finite field operations. A finite field, sometimes named "Galois field" with the shorthand notation GF, is a *field* containing a finite number of elements. A field, in the sense of mathematics, is a set on which addition, subtraction (inverse-addition), multiplication, and division (inverse-multiplication) are defined along with the additive identity (usually written as "0") and multiplicative identity (usually written as "1"). The following field axioms are satisfied by the addition and the multiplication operations. Let a, b, and c be three arbitrary elements in a field, a field satisfies

- Associativity of addition and multiplication.

$$a + (b + c) = (a + b) + c \qquad\qquad a \cdot (b \cdot c) = (a \cdot b) \cdot c$$

- Commutativity of addition and multiplication.

$$a + b = b + a \qquad\qquad a \cdot b = b \cdot a$$

- Distributivity of multiplication over addition.

$$a \cdot (b + c) = (a \cdot b) + (a \cdot c)$$

The number of elements in a finite field is called the *order* of the field. For example, the binary base field in the butterfly example is a $GF(2)$, a finite field of order 2, and XOR is the addition operation over $GF(2)$.

In this work, our system codes over $GF(2^8)$. To perform linear coding over a base field with a larger size, we map the base field to a finite field with the same order. The key step in the mapping is to determine the two arithmetic operations: addition and multiplication. The addition can be done by the bit-wise XOR operation, and the multiplication is chosen as the one used in the Advanced Encryption Standard [43].

CHAPTER 3

SYSTEM OVERVIEW

We give an overview of CodedBulk in this chapter. The chapter starts with the design opportunities and challenges, followed by the design decisions. An architecture overview of CodedBulk is given at the end of the chapter.

3.1 Opportunities

The inter-datacenter networks exhibit some special characteristics that differentiate them from other router-based networks. We discuss in the followings the new design opportunities resulting from those characteristics.

Delay-tolerant bulk transfers Over an inter-datacenter network, bulk transfers are performed by large-scale service providers across data centers to shorten content delivery latency, improve fault tolerance, increase data availability, and achieve load balancing. Those bandwidth demanding but delay tolerant tasks are often scheduled in advance and carried by low-priority bulk traffic.

The aforementioned nature of the bulk traffic allows new trade-offs in the context of inter-datacenter networks. In particular, techniques that minimize the bandwidth to transfer bulk traffic while not inflating the latency significantly are highly desirable.

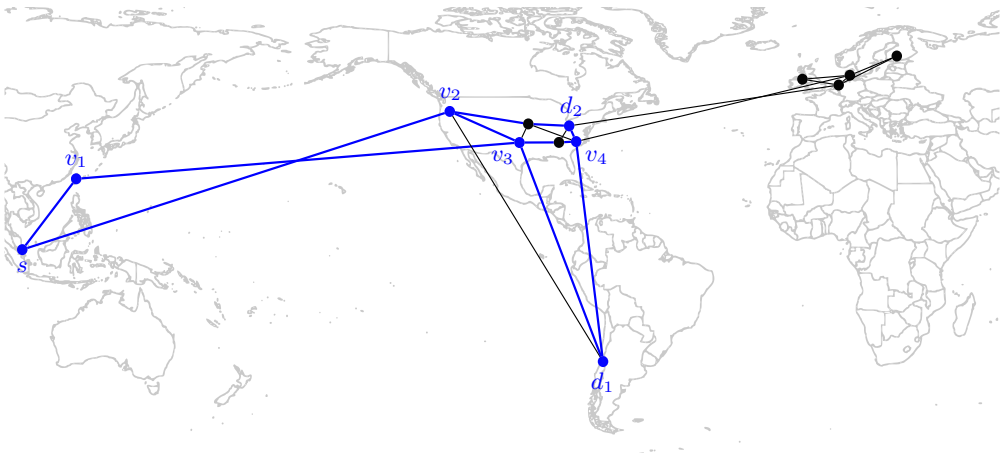

Figure 3.1: Google's SDN-enabled inter-datacenter network, B4, is a cross-continental wide-area network connecting 13 data centers. We mark in blue a subnetwork as the 7-*node example* henceforth for concept illustration.

Small-scale programmable networks Contrary to the huge number of nodes in the Internet and the wide-area networks formed by multiple ISPs, inter-datacenter networks comprise much fewer cites, only tens of data centers. For example, Figure 3.1 shows Google's B4 inter-datacenter network, which consists of 13 nodes worldwide. Such a small scale allows solving complex optimization problems that would otherwise lead to scalability concerns in data centers with hundreds or thousands of switches. In addition, inter-datacenter networks like B4 [6] and SWAN [7] are controlled by a single entity and often software-defined enabled, thus making it easy to program the network by pre-configuring routes and coding functions to efficiently implement coded bulk transfers.

Resource-rich intermediate nodes Unlike data center networks where nodes along the path between the source and the destination are resource-constrained switches, each node in an inter-datacenter network is a data center with abundant computation and storage capacity. As a result, we can leverage the intermediate nodes to buffer and code data before forwarding it at line rate, which

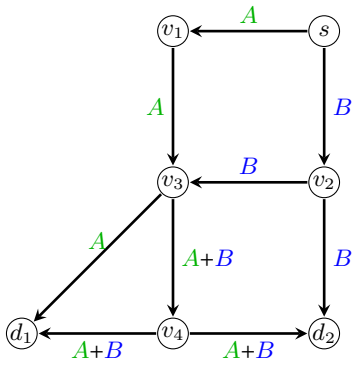

Figure 3.2: A closer look of the 7-node topology from Figure 3.1. Assuming each link has a unit capacity, we consider a multicast flow with source s and two destinations d_1 and d_2. This 7-node example demonstrates how a coding scheme can be deployed to allow both destinations receive two unit symbols, A and B, concurrently in a network with min-cut capacity 2. The symbols are merged at node v_3 and decoded at the destinations.

is impossible using commodity switches in data centers. By doing so, we can trade-off a little computation and storage resources for less bulk traffic bandwidth through network coding. For instance, the intermediate node v_3 in Figure 3.2 buffers the symbols received from v_1 and v_2 and forwards the merged symbols to v_4 and d_1, which is not feasible if v_3 is a commodity switch instead of a data center.[1]

3.2 Challenges

Multiple bulk transfers Traditional network coding literature examines the case of a single source multicast traffic sending traffic over an empty network. However, an inter-datacenter network can have multiple concurrent bulk transfers at the same time. The coexistence of multiple bulk transfers leads to the rate

[1]It is also possible to achieve per destination min-cut capacity in the 7-node example by routing and mirroring. Here we use the 7-node example for simpler coding scheme illustration.

sharing issues that are not well-studied in the network coding literature. As a result, we need to address the rate sharing issues among multiple coded bulk transfers in our design, which can involve throughput, fairness, or utilization concerns.

Non-uniform bandwidth availability An inter-datacenter network has not only the low-priority bulk transfers but also the high-priority interactive traffic. In particular, B4 carries three main kinds of traffic [6]: high priority (and latency sensitive) interactive traffic comprising copying of end-user application data mainly for higher availability, lower priority traffic linked with retrieval of remotely stored data for computational purposes, and the lowest priority (and relatively most latency agnostic) bulk traffic mainly comprising of large-scale copies of datasets across the sites for synchronization among the data centers. This layered priority design grants bandwidth accordingly and results in varying bandwidth for the lower-priority traffic, especially the bulk transfers. Such a non-uniform bandwidth availability can hurt the performance of the designed coding scheme, which we illustrate in Figure 3.3.

Figure 3.3(a) shows the fully-utilized 7-node network using the coding scheme in Figure 3.2. The co-existing high-priority interactive traffic shares some link with the coded bulk traffic and causes the under-utilization of the other links as in Figure 3.3(b). We name this phenomenon the *blocking effect*, which will be discussed in details in Chapter 6.

Asymmetric transmission latency Non-uniform delay across paths is not considered in traditional network coding literature. Disregarding propagation delay and processing time, the network is deemed fully synchronized, which al-

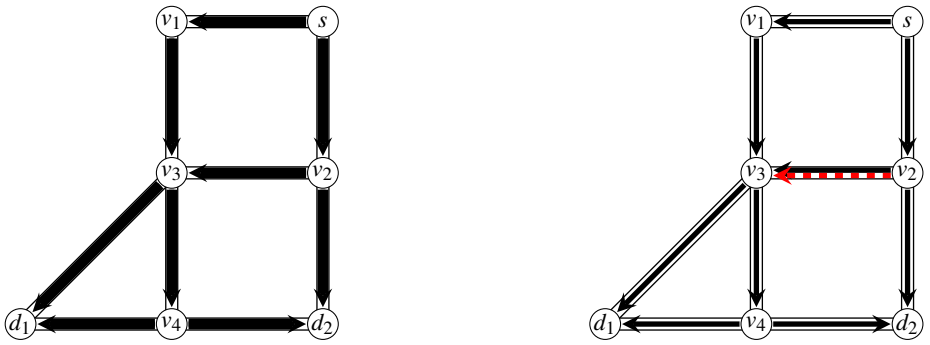

(a) The coded traffic fully utilizes all available bandwidth.

(b) The existence of interactive traffic (red dashed arrow) leads to bandwidth under-utilization.

Figure 3.3: In the presence of interactive traffic, the available bandwidth for the coded bulk traffic decreases, which leads to under-utilization of non-congested links.

(a) Google's B4.

(b) Microsoft's SWAN

Figure 3.4: Inter-datacenter networks spread worldwide. Different links connecting different pairs of cites can lead to different transmission latency, which prevents the network being perfectly synchronized.

lows the symbols being coded and forwarded upon arrival. An inter-datacenter network, however, operates asynchronously in practice due to asymmetric transmission latency among the paths. For instance, Figure 3.4 shows the inter-datacenter network topologies of Google's B4 (Figure 3.4(a)) and Microsoft's SWAN (Figure 3.4(b)), in which the geographically separated cites are connected by links of various lengths and delays. As a result, the symbols collected from distinct cites undergo different delays that prevent them from being received at the same time for coding.

3.3 Design Decisions

We design CodedBulk to allow minimal-change integration to existing inter-datacenter networks, such as B4 [6] and SWAN [7]. To start with, we elaborate the design features of the existing inter-datacenter networks.

Existing inter-datacenter designs like B4 [6] and SWAN [7] leverage centralized SDN-based traffic engineering to improve the average inter-datacenter link utilization. The key motivating factor behind the approach is twofold – First, complete programmability is possible as all data centers belong to one same entity end-to-end from physical infrastructure to application software; Second, the scalability concerns about centralization are ruled out by the small scale of the inter-datacenter networks consisting of only tens of the data centers. These designs also introduce a prioritized framework for the interactive (high priority) and the bulk (low priority) traffic. Moreover, their centralized routing mechanisms periodically find the optimal paths for the flows depending upon the traffic and program the switches across all the sites in a synchronized manner.

We design CodedBulk to exploit the existing features, explore the new opportunities, and handle the aforementioned challenges, and our design decisions are summarized in Table 3.1. In particular, CodedBulk employs network coding on top of the network/transport layer functionalities provided by these SDN-based approaches. Hence, routing and transport for the non-coded interactive traffic remain unchanged from the underlying network design. For the coded bulk traffic, CodedBulk introduce the store-and-forward model to tackle the asymmetric transmission latency. Multi-hop TCPs are used to perform load balancing among multiple coded sessions. Taking the pre-scheduled bulk ses-

Table 3.1: Design decisions of CodedBulk with their corresponding rationale and implementation challenges. The challenges will be addressed in Chapter 6.

Design Decision	Rationale	Challenges
Network coding	Each node is a data center of rich computation resources.	Computational overhead at intermediate nodes.
Store-and-forward model	Each node is a data center having plenty of storage. Bulk traffic is delay-tolerant.	Data accumulation at intermediate nodes.
Multi-hop TCP	Fair sharing among multiple bulk traffic is done on a per-link basis. Coding above the transport layer leverages existing lower layer network functions.	End-to-end flow rate control.
Centralized coding scheme computation	SDN-enabled network allows centralized computation and deployment of the coding scheme. Bulk traffic is pre-scheduled.	Non-uniform bandwidth availablility.

sions into account, the corresponding coding schemes are generated by the centralized SDN controller which maintains a full view of the network topology.

The design decisions accompany some implementation challenges: Network coding imposes computational overhead at each node; the store-and-forward model would lead to data accumulation at an intermediate node when its available upstream and downstream bandwidth is imbalanced; Breaking end-to-end TCP into multi-hop TCPs requires an appropriate rate control mechanism to orchestrate the resulting subconnections; Non-uniform bandwidth availability can obsolete the pre-computed coding scheme. We will discuss our approaches to those challenges in Chapter 6.

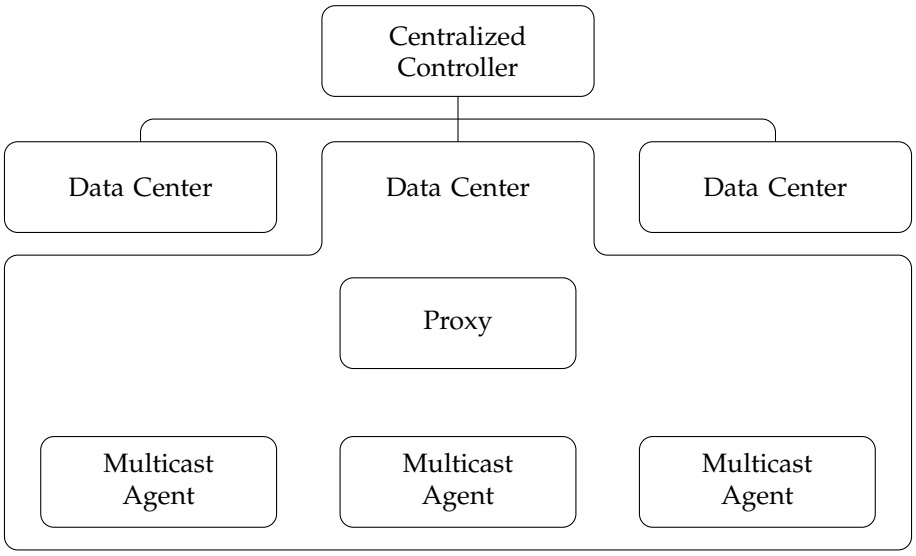

Figure 3.5: Architecture overview of CodedBulk.

3.4 CodedBulk in a Nutshell

In Figure 3.5, we provide a brief architecture overview of CodedBulk. CodedBulk consists of three main parts in an inter-datacenter network: the multicast agents, the proxies, and the centralized controller.

Each multicast agent handles one multicast bulk transfer. When a data center issues a multicast task, it creates one corresponding multicast agent sender. The multicast agent sender will inform the destination data centers to create the multicast agent receivers. Meanwhile, it notifies the centralized controller of the source and the destinations of the bulk transfer for coding scheme computation.

Once the coding scheme is established, the multicast agent forwards the bulk traffic for coding to the proxy at the node. Logically, each data center has one proxy that performs the network coding functions installed by the centralized controller. The proxy establishes multi-hop TCPs with and forwards coded traffic to the proxies at the neighboring data centers. The proxy also decodes the

information and dispatches it to the corresponding multicast agent receivers.

The centralized controller maintains a global view of the underlying inter-datacenter network, collects the bulk traffic information from the multicast agents, computes the coding schemes, and deploys the coding functions to the proxies.

We will scrutinize the architectures of the multicast agent and the proxy in Chapter 4 and elaborate our coding algorithm at the centralized controller in Chapter 5.

CHAPTER 4

DESIGN DETAILS

The main task of CodedBulk is to improve the throughput of bulk transfer. We leverage network coding to approach such goal. Network coding reduces the bandwidth requirement of a multicast traffic and hence min-cut capacity can be achieved at each destination in theory [11]. In this chapter, we present our system design to incorporate network coding into inter-datacenter bulk transfer.

We begin the chapter with the two basic entities in the system: *multicast agent* and *TCP proxy*. The TCP proxies establish hop-by-hop TCPs and we introduce *flow identifier* to identify the connections. On top of the TCP proxies, we develop the coding functionality. At each proxy, we install a *codec manager* that aggregates the *codecs*. Codecs are described by the *code maps* to merge the incoming data streams.

In the following context, we let $G = (V, E)$ be the underlying network topology, where V is the set of nodes (data centers) and E is the set of the edges. Without further specification, edge capacity is included in the topology information at each edge. A path is defined as a single-path route in the network, and we use the terms "path" and "route" interchangeably without confusion.

4.1 Multicast Agent

A multicast flow disseminates data to a set of destinations through a *multicast agent (MA)*, which handles the communication between the source and the destinations. In practice, the data of a multicast flow can be generated by an application, and the multicast agent can be a socket, an interface, or the application

itself that supports multicast functionality. A multicast agent consists of two sides: the sender side and the receiver sides, and we refer to the sender side by MA^t and the receiver sides by MA^r.

MA^t sends data to each MA^r through a set of *multicast path sets (MPSs)*. An MPS consists of one path to each destination. Although the edges occupied by the paths in an MPS form a tree, we still present such multicast structure in terms of a set of paths rather than a tree, which allows us to assign two different symbols to two different paths sharing the same edge later in the chapter.

For each path in an MPS, MA^t and MA^r establish a TCP connection on it as in Figure 4.1. As such, MA^t can send data through a specific path by sending it through the corresponding TCP. The TCPs also limit the data rate of an MPS. MA^t sends data through the paths in an MPS with a rate no more than the smallest throughput within the corresponding TCPs.

When multiple MPSs are available for an MA^t, the MA^t can multicast data through the MPSs[1]. Regarding the load balancing among those MPSs, this work relies on the convergence of the TCPs to determine a "fair share" for each MPS.

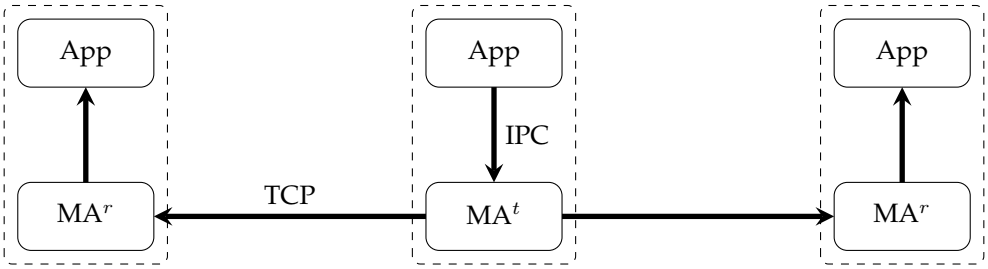

Figure 4.1: Multicast agents disseminate data from a source to corresponding destinations. Dashed squares represent the nodes.

The MPSs can be given by some existing routing algorithms. In CodedBulk,

[1]Some sequence reordering mechanisms might be needed for MA^r to guarantee in order delivery as in MPTCP [44].

an SDN centralized controller is in charge of generating MPSs for multicast flows. The multicast agents first report their source and destinations to the SDN centralized controller. The controller will generate a set of MPSs for each multicast flow by Algorithm 1 and install those sets of MPSs to the corresponding multicast agents. Each multicast agents then send data through the assigned MPSs.

Algorithm 1 generates the MPSs by first finding a set of routes to each destination. Those routes are explored by a greedy path exploration algorithm (Algorithm 2), which keeps searching for a path until no path can be found. Algorithm 2 starts with a full network topology, repeatedly finds an available path in a greedy fashion, removes the path with maximum available bandwidth, and terminates when the source is separated from the destination.

Algorithm 1: Multicast path set generation

Input: The network topology $G = (V, E)$. The multicast flow f with source $s \in V$ and the destinations $D \subset V$ where $s \notin D$.
Output: The set of MPSs $\mathcal{M}_s^D$.

1: $\mathcal{M}_s^D \leftarrow \emptyset$.
2: Obtain P_{sd} using Algorithm 2 for all $d \in D$.
3: **while** P_{sd} is non-empty for all $d \in D$ **do**
4: Let p_{sd} be a path in P_{sd} for all $d \in D$.
5: Generate an MPS $M = \bigcup_{d \in D} \{p_{sd}\}$ and add it to $\mathcal{M}_s^D$.
6: $P_{sd} \leftarrow P_{sd} \setminus p_{sd}$ for all $d \in D$.
7: **end while**
8: **return** $\mathcal{M}_s^D$.

4.2 TCP Proxy

Performing network coding requires computation at each node. We perform the computations at the application layer by introducing a proxy at each data

Algorithm 2: Greedy path exploration

Input: The network topology $G = (V, E)$. The source $s \in V$ and the destination $d \in V$.

Output: The set of distinct paths P_{sd} between s and d.

1: $P_{sd} \leftarrow \emptyset$.
2: Let G' be a copy of G.
3: **while** There exists a path p from s to d with non-zero bandwidth in G' **do**
4: Find the maximum available bandwidth for p and subtract it from the capacity of the edges that p goes through from G'.
5: $P_{sd} \leftarrow P_{sd} \cup \{p\}$.
6: **end while**
7: **return** P_{sd}.

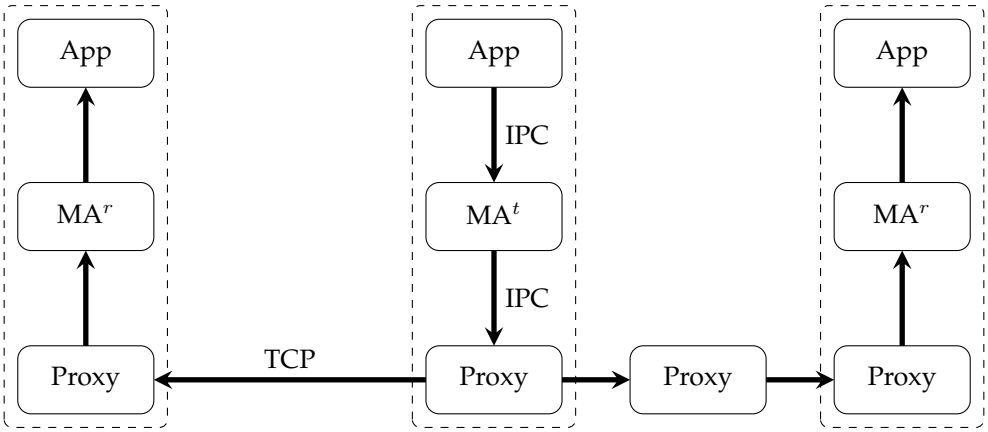

Figure 4.2: Proxies receive data from a multicast agent sender and multicast it to the destinations. The data is coded hop-by-hop and forwarded by the proxies.

center. As the proxy operates at the application layer, the ordering and loss issues of the data stream is handled by the underlying transport layer, and the coding is performed on the data.

Without proxies, MA^t sends to each MA^r directly. We introduce proxies such that MA^t sends data to the proxy at the source using inter-process communication (IPC) and relies on the proxies to deliver the data to each MA^r as in Figure 4.2. One thing noticeable is that a node can have multiple MAs, but there is only one proxy at each node.

Figure 4.3 shows the architecture of a proxy. In this work, we consider TCP proxies, which break an end-to-end TCP connection into multiple hop-by-hop TCP connections. Each hop-by-hop TCP connection lies between a pair of neighboring proxies. Such scheme is also known as "split TCP" [45].

A proxy contains a *codec manager* that manages a set of registered *codecs*. Once new data is received, the proxy stores the data and calls the codec manager to match the data to the corresponding codecs.

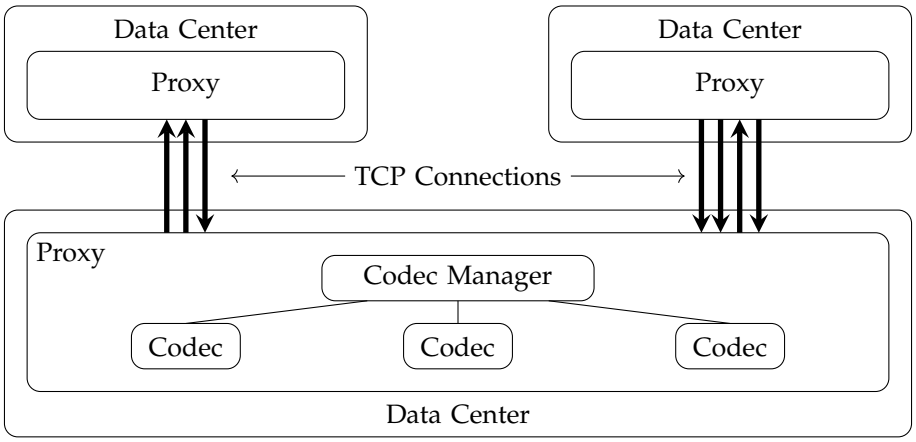

Figure 4.3: Proxy architecture.

4.3 Hop-by-Hop TCP and Flow Identifier

Given a simple path p_1, we partition it into hop-by-hop TCP connections and mark those connections with a *flow identifier (FI)* p_1. In this work, FI is a 4-byte integer. Each node will have at most one TCP sender and one TCP receiver of the same FI, we mark them FI^t and FI^r, respectively. With a slight abuse of notation, we refer to a path by its FI and vice versa.

To setup the hop-by-hop TCP connections, the centralized controller specify

the next hop for each FI at each proxy. This procedure is similar to installing a routing rule at a router. Although the next hop information is available, the FI^t is not established until the proxy needs to forward data to it.

As to how hop-by-hop TCP connections will be established, the proxy listens to a predetermined TCP port for hop-by-hop TCP establishment. When a TCP client at the remote, or an FI^t, connects to the port, the proxy creates a TCP server that expects FI as the first message, followed by the data stream. Once the TCP connection is established, the client sends its FI to the server and the server will be assigned as FI^r. As such the FI^t and FI^r pair is connected, and the data will be streamed from FI^t to FI^r.

We deem each byte in the data stream a *symbol*, which is the basic coding unit in network coding theory. In the literature, a symbol is represented by a single bit [35], an 8-bit, or a 16-bit unit [34]. We choose one byte as the basic unit, since finite field arithmetic operations over $GF(2^8)$ is a building block for the well-known Advanced Encryption Standard (AES) [43].

4.4 Codec Manager

Each proxy has one *codec manager* which aggregates the available codecs and provides a unified interface for coded data stream handling. Whenever a proxy receives a data stream from some FI^r, it consults with its codec manager to determine if some codecs require the data stream. If so, the data stream is distributed to the required codecs by the codec manager. Otherwise, the data stream is discarded as if no rule routes it from the inport to an outport in a router.

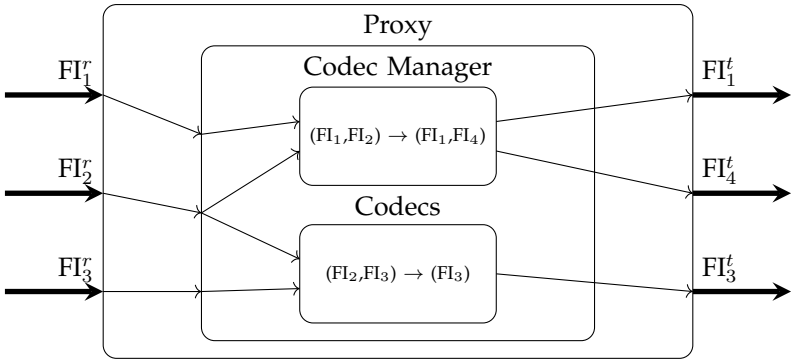

Figure 4.4: Codec manager forwards data stream from FI^r to the corresponding codecs. The output data stream is then sent to the FI^t.

The above workflow is demonstrated in Figure 4.4. Comparing with a router, registering a codec at the codec manager is analogous to installing a routing rule at the routing table. In that sense, coding is similar to routing. The difference is that routing does not generate additional packets, and each packet can only be forwarded according to one rule (or one sequence of rules). In contrast, one data stream can "match against" several codecs, and each codec can produce multiple output data streams.

4.5 Codec

As shown in Figure 4.4, the codec manager maintains a set of codecs that code the input data streams to be output data streams. In this work, the codecs are registered at the codec manager by the centralized controller. The controller computes the codes for each proxy in the form of *code maps* and the codecs are created accordingly.

A codec performs coding based on its code map. A code map is defined by the input FI^rs, the output FI^ts, and the code matrix that describes the linear map

from the inputs to the outputs. We illustrate how a code map is written in the following simple example.

Example 4.5.1 (Code Map: Simple Forwarding)**.** *One of the simplest code maps is forwarding. Given a path p_1, the following code map takes the input symbol from the input (TCP receiver) with FI p_1, multiplies it by identity, and sends it to the output (TCP sender) with FI p_1:*

$$\textit{mapping: } (p_1) \to (p_1),$$
$$\textit{code matrix: } \begin{bmatrix} 1 \end{bmatrix}.$$

If we have another forwarding code map that forwards FI p_1 to FI p_2, together with the above one, we can duplicate the symbol received from the input with FI p_1 to the outputs with FI p_1 and p_2.

To demonstrate how we can use code maps to realize desired codes, we revisit the 7-node example that is introduced in Chapter 3.

Example 4.5.2 (7-node Example Revisit)**.** *Consider the 7-node example in Figure 3.1. Suppose we are given two MPSs as in Figure 4.5(a). The green MPS consists of paths p_1 and p_3, and the other has p_2 and p_4. Our goal is to construct the code maps to achieve the codes in Figure 4.5(b), in which A is a symbol sent through the green MPS and B is a symbol carried by the blue.*

We start with the paths partitioned into hop-by-hop TCP connections in Figure 4.5(c), and then we design code maps to fit symbols to the TCP connections.

The simplest code map would be the forwarding code map at v_1. The code map takes symbol A from ${p_1}^r$ and forwards it to ${p_1}^t$. We can also derive the code maps at v_2 and v_4

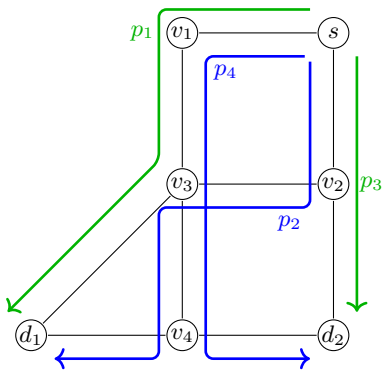

(a) 2 given MPSs consist of 4 paths.

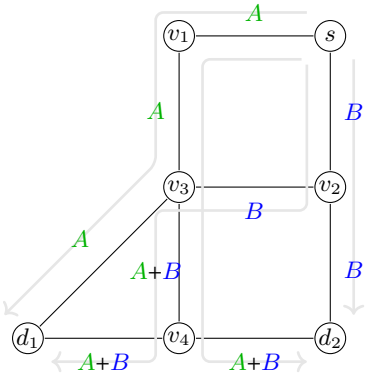

(b) The desirable codes.

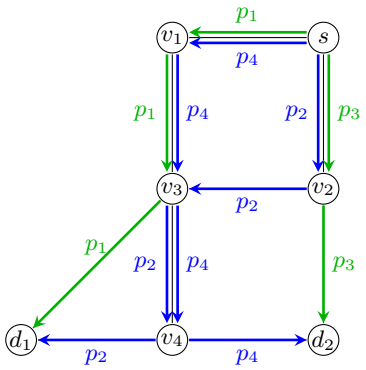

(c) Hop-by-hop TCP connections and their FIs.

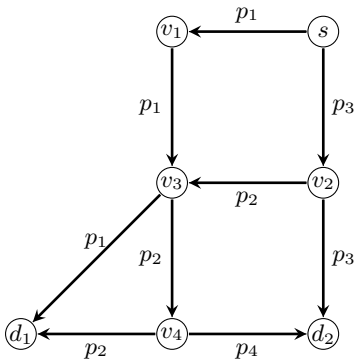

(d) Established TCP connections.

Figure 4.5: The 7-node example. Given the MPSs and the desirable codes, we can derive the corresponding code maps to realize the codes. The derived code maps establish only a subset of the available hop-by-hop TCP connections.

easily. As shown in the previous example, duplication can be done by two forwarding code maps.

The code maps at the source s involves selection. s selects only A to send to ${p_1}^t$ (and only B to ${p_3}^t$), which is equivalent to multiplying the symbols from ${p_1}^r$ and ${p_4}^r$ by identity and zero, respectively, and summing the results together. Such operation can be written as a matrix multiplication, which leads to the code map in Table 4.1. Similarly, merging symbols, or linear combining symbols, can also be expressed by a

Table 4.1: The code maps of the registered codecs at each node in the 7-node example.

Node	Code Maps	
s	$(p_1, p_4) \rightarrow (p_1)$,	$\begin{bmatrix} 1 & 0 \end{bmatrix}$
	$(p_2, p_3) \rightarrow (p_3)$,	$\begin{bmatrix} 1 & 0 \end{bmatrix}$
v_1	$(p_1) \rightarrow (p_1)$,	$\begin{bmatrix} 1 \end{bmatrix}$
v_2	$(p_3) \rightarrow (p_2)$,	$\begin{bmatrix} 1 \end{bmatrix}$
	$(p_3) \rightarrow (p_3)$,	$\begin{bmatrix} 1 \end{bmatrix}$
v_3	$(p_1, p_2) \rightarrow (p_1)$,	$\begin{bmatrix} 1 & 0 \end{bmatrix}$
	$(p_1, p_2) \rightarrow (p_2)$,	$\begin{bmatrix} 1 & 1 \end{bmatrix}$
v_4	$(p_2) \rightarrow (p_2)$,	$\begin{bmatrix} 1 \end{bmatrix}$
	$(p_2) \rightarrow (p_4)$,	$\begin{bmatrix} 1 \end{bmatrix}$
d_1	$(p_1, p_2) \rightarrow (p_1, p_2)$,	$\begin{bmatrix} 1 & 0 \\ 1 & 1 \end{bmatrix}$
d_2	$(p_3, p_4) \rightarrow (p_3, p_4)$,	$\begin{bmatrix} 1 & 1 \\ 1 & 0 \end{bmatrix}$

matrix multiplication. One such case is at v_3, the symbols from ${p_1}^r$ and ${p_2}^r$ are combined and sent to ${p_2}^t$.

Deriving the code maps at the destinations is a little more involved. At d_1, we want to decode A for ${p_1}^t$ and B for ${p_2}^t$, while we receive A from ${p_1}^r$ and $A + B$ from ${p_2}^r$. Therefore, we can express the relationship by the following equation

$$\begin{bmatrix} \text{symbol from } p_1^r \\ \text{symbol from } p_2^r \end{bmatrix} = \begin{bmatrix} 1 & 0 \\ 1 & 1 \end{bmatrix} \begin{bmatrix} \text{symbol to } p_1^t \\ \text{symbol to } p_2^t \end{bmatrix}.$$

As a result, the code map can be written as

$$\textit{mapping: } (p_1, p_2) \rightarrow (p_1, p_2),$$

$$\textit{code matrix: } \begin{bmatrix} 1 & 0 \\ 1 & 1 \end{bmatrix}^{-1} = \begin{bmatrix} 1 & 0 \\ 1 & 1 \end{bmatrix}.$$

And the code map at d_2 can be obtained in the same way.

At this point, we have learned how to derive all the code maps in Table 4.1. We remark that not all the hop-by-hop TCP connections will be established and utilized by the derived code maps: only the ones in Figure 4.5(d) will be used.

As demonstrated in the example above, we don't and need not differentiate between coding and decoding. Essentially, they are the same: multiplying the symbols by a code matrix.

CHAPTER 5

CODING ALGORITHM

As to how the code maps can be generated, we develop a *cycle-aware coding algorithm* in this chapter. It computes the code maps at each node by greedily merging the given paths. The purpose of the algorithm is to produce codes using the given paths from any existing network layer. Since no constraint is imposed on the given paths, cycles may exist among them, which paralyze existing coding algorithm. Our cycle-aware coding algorithm takes such situations into account and remains effective even in the presence of cycles.

In the literature, most of the network coding algorithms aim to associate a symbol with each edge. In this work, however, we assign a symbol to each hop-by-hop TCP connection. Since an edge can carry several hop-by-hop TCP connections, several symbols can be sent through the same edge, which allows superposition of different coded flows.

Besides the edge-based code generation, most network coding algorithms, including the well-known polynomial-time coding algorithm [33], require the knowledge of the network to both generate paths (or sometimes trees) and the corresponding symbols on each edge for the multicast session. In our design, we develop an algorithm that takes only predetermined MPSs as the input, and generate the codecs at each node that leads to the corresponding symbols for each hop-by-hop TCP connections.

The coding algorithm we develop in this work, named *cycle-aware coding algorithm* (Algorithm 6), is inspired by [33]. However, our algorithm is more general than [33] as

- the network topology is not needed as our algorithm assumes the MPSs are given and it will not jointly determine the paths and the codes.
- our algorithm does not require the given paths to be edge-disjoint and a topological order of the network topology to exist. It assigns symbols to hop-by-hop TCPs instead of edges and resolves the dependency deadlock when the given paths form cycles.

5.1 Codec Generation

Given the MPSs, we generate the codecs at each node by merging the paths together as inspired by [33]. Assuming that each MPS disseminates one symbol to the destinations, we merge paths while maintaining all the symbols "decodable" at each destination.

For a multicast flow with the source s and the set of destinations $D \subset V$, let $\mathcal{M}_s^D$ be the given set of MPSs consisting of $|\mathcal{M}_s^D|$ MPSs. We express one original symbol for each MPS by a unit vector of dimension $|\mathcal{M}_s^D|$, called a *content vector*. As such, linear combinations of the original symbols, or the coded symbols, can be written as $|\mathcal{M}_s^D|$ dimension content vectors. We associate each path in an MPS $M \in \mathcal{M}_s^D$ with the corresponding unit content vector.

Let P_{sd} be the set of the paths from s to d and P_v be the set of paths going through node v in all the MPSs. We collect the content vectors of the paths in P_{sd} as the rows in the *basis matrix* C_{sd} at each destination d. For each path p, we denote by c_p the last content vector assigned to its edges and by i_p the *information carrying FI*. Information carrying FI is the FI that currently carries the content vector, initially set as the FI of the path itself.

Algorithm 3: Codec generation for node v

Input: The set of paths P_v and the basis matrices C_{sd} for all $d \in D$.
Output: Updated basis matrices C_{sd} for all $d \in D$.

1: **while** $P_v \neq \emptyset$ **do**
2: Select the paths from P_v that go through the same next edge after v but with different destinations, and store them in P.
3: Use the method in [33] to find a vector $u = \sum_{p \in P} \eta_p c_p$ such that C_{sd} for all $d \in D$ are all full-rank (invertible) after replacing c_p with u for all $p \in P$.
4: Let $P = \{p_1, p_2, \ldots, p_n\}$. Register a codec at v with the code map

$$\text{mapping: } (i_{p_1}, i_{p_2}, \ldots, i_{p_n}) \rightarrow (p_1),$$
$$\text{code matrix: } \begin{bmatrix} \eta_{p_1} & \eta_{p_2} & \cdots & \eta_{p_n} \end{bmatrix}.$$

5: $c_p \leftarrow u$ and $i_p \leftarrow p_1$ for all $p \in P$.
6: $P \leftarrow P \setminus P_v$.
7: **end while**
8: **return** C_{sd} for all $d \in D$.

We summarize in Algorithm 3 how the codecs are generated at each node v, which will be the building block of our cycle-aware coding algorithm (Algorithm 6).

5.2 Dependency Deadlock Resolve

Algorithm 3 can generate the codecs at a node v if the codecs have been decided for all nodes prior to v of the paths in P_v. In [33], the authors assume the existence of a topological order in the network, and generate the codes accordingly. Generating codecs under a topological order ensures all prior nodes have been processed before a node is under consideration.

In our setting, it is possible that a topological order does not exist because the network topology is not necessarily directed acyclic. Instead, an inter-

datacenter network usually consists of bidirectional links. As a result, the underlying network layer can give MPSs that contain paths forming cycles. In other words, the paths of the given MPSs do not hold a topological order, and we aim to code such given MPSs as well.

A cycle tangles a pair of nodes to depend on each other. We call such issue a *dependency deadlock*. In the following example, we explains how cycles create a dependency deadlock and why we can't simply ignore the cycle.

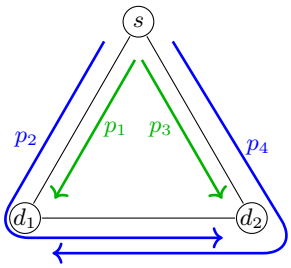

(a) The paths p_2 and p_4 forms a cycle on edge (d_1, d_2).

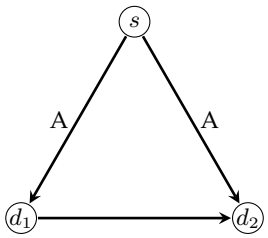

(b) Sending traffic on the maximum capacity directed subgraph achieves throughput 1.

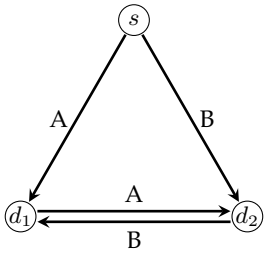

(c) The optimal throughput involves the utilization of the bandwidth in both directions.

Figure 5.1: A cyclic network with s multicasting to d_1 and d_2.

Example 5.2.1 (Cycles and Dependency Deadlock)**.** *The simplest dependency deadlock example would be coding over a triangular network. Consider three nodes s, d_1, and d_2 in Figure 5.1. Suppose the two given MPSs are*

$$MPS1 : p_1 = (s, d_1), \quad MPS2 : p_2 = (s, d_2, d_1),$$

$$p_3 = (s, d_2). \qquad p_4 = (s, d_1, d_2).$$

The MPSs are marked green and blue in Figure 5.1(a).

After the codecs at s are computed, the codes for all the hop-by-hop TCPs on (s, d_1) and (s, d_2) are determined. Meanwhile, we encounter a dependency deadlock when choosing the next node to code. If we choose d_1 as the next node, since the code on (d_2, d_1) is not yet decided, we can't compute the codec at d_1. Similar problem is encountered if we choose d_2 to code first.

One way to deal with the cycles is to ignore them. For instance, one might extract the maximum capacity directed subgraph from the original network first and send traffic only upon it. However, such approach would lead to performance degradation as shown in Figure 5.1(b).

To resolve this dependency deadlock, we can choose one node arbitrarily, say d_2, and force all the incoming paths forwarding the latest decided symbols to the node. In this case, we ask p_4 to forward through (d_2, d_1) the same symbol as the symbol on (s, d_2). Therefore, the symbol on the hop-by-hop TCP (d_2, d_1) is decided (which is $\boldsymbol{B}$ in this case), and the codecs at d_1 can be computed. In this way, we can send the traffic that achieves the min-cut capacity per destination as in Figure 5.1(c).

The optimal coding scheme in Example 5.2.1 can be realized by pure routing and one might suspect if pure routing is sufficient when cycles are presented. In the following example, we show that we must leverage both directions of a cycle to reach the optimal performance.

Example 5.2.2 (Insufficiency of Routing under Cycles)**.** *Consider a tweaked butterfly example in Figure 5.2. One multicast flow sends from s to three destinations d_1, d_2, and d_3. A bidirectional link (d_1, d_3) provides unit capacity for both directions. The optimal coding scheme involves merging the symbols at v_3 and utilizes both directions*

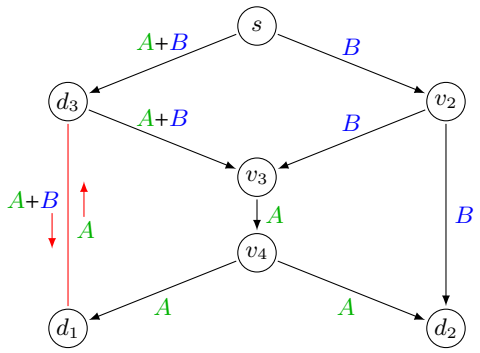

Figure 5.2: Routing is insufficient in achieving the per destination min-cut capacity in a unit capacity network consisting of some undirected links. A multicast flow sends from s to three destinations d_1, d_2, and d_3. The red line represents an undirected link, and the optimal coding scheme both performs coding at v_3 and utilizes the bandwidth of (d_1, d_3) bidirectionally.

of (d_1, d_3) *to achieve per destination min-cut capacity* 2. *If one direction is neglected, the min-cut capacity becomes* 1, *which implies that no coding scheme would be able to achieve throughput more than* 1 *per destination.*

This cycle issue is also observed in the network coding literature [11, 46]. To handle the cycles, convolutional network coding is adopted and proven optimal theoretically [46]. Convolutional network coding takes into account the delay of the links and cross-codes the symbols that belong to different time steps. As a result, the computation of the convolutional codes requires precise knowledge of the network delay; the coding scheme will be time-dependent; the codec architecture would be much more complicated; and the existing algorithm [46] is much harder to implement than [33]. Therefore, we introduce a simple tweak into [33] that allows our simple codec architecture to deal with the dependency deadlock without needing the precise delay information.

As in the above examples, the idea of dealing with dependency deadlock is

to "skip" some nodes in some paths to restore the topological order. To do so, we introduce a *node pointer* n_p for each path p. The node pointer points to the first node in path that no codec has been installed regarding the symbol sent on the path. In other words, a node pointer specifies the node at which new codecs should be installed for the path. By definition, n_p points to the source node s in the beginning for all paths.

To decide which node to generate codes, we check if there exists a node that the paths going through it have all the prior nodes processed. If so, the node will be chosen to generate codecs. Otherwise, we choose a node arbitrarily and skip all prior non-processed nodes for each path by installing a forwarding codec. The procedure is summarized in Algorithm 4. We remark that Algorithm 4 results in a topological order whenever there exists one.

Algorithm 4: Finding the next node to code

Input: The set $\mathcal{P}$ which consists of non-empty P_v.
Output: The next node to code v.

1: **if** There exists v where $P_v \in \mathcal{P}$ such that $n_p = v$ for all $p \in P_v$ **then**
2: **return** v
3: **end if**
4: Pick $P_v \in \mathcal{P}$ for some v.
5: **for** $p \in P_v$ **do**
6: **while** $n_p \neq v$ **do**
7: $P_{n_p} \leftarrow P_{n_p} \setminus p$. If $P_{n_p} = \emptyset$, remove it from $\mathcal{P}$.
8: Register a forwarding codec at n_p with the code map

$$\text{mapping: } (i_p) \to (p),$$
$$\text{code matrix: } \begin{bmatrix} 1 \end{bmatrix}.$$

9: $i_p \leftarrow p$.
10: Point n_p to the next hop.
11: **end while**
12: **end for**
13: **return** v

Algorithm 4 can be viewed from another angle. Consider again the 3-node

cyclic network in Example 5.2.1. In Figure 5.1(c), the node d_2 is chosen to be "skipped," which can be deemed as if we replace the link (d_2, d_1) by installing a dummy mirroring node on (s, d_2). Such operation is depicted in Figure 5.3(a). After the transformation, the network is acyclic with a topological order. According to the topological order, we can find the codecs at each node by Algorithm 3.

(a) The cycle can be removed by adding a dummy mirroring node on the upstream link (s, d_2).

(b) Adding the dummy node makes the network acyclic, and hence the coding scheme can be found by Algorithm 3 according to a topological order.

Figure 5.3: Algorithm 4 resolves dependency deadlock by breaking the cycles arbitrarily. Alternatively, the operation can also be interpreted as installing auxiliary dummy nodes.

5.3 Cycle-Aware Coding Algorithm

Combining the codec generation (Algorithm 3) and the next node finding (Algorithm 4) procedures, we propose our cycle-aware coding algorithm in Algorithm 6. To improve readability, we specify the initialization setup in Algorithm 5.

In our system, the centralized controller collects the source and the destinations of the multicast flows in the network and utilizes Algorithm 1 to route

them through MPSs according to the sensed network topology. The generated MPSs are then fed to Algorithm 6 to register codecs at each node.

After generating the codes for all the nodes besides the destinations, we derive the code matrices for the decoding code maps at each destination as in line 8 of Algorithm 6. Notice that C_{sd} is invertible since Algorithm 3 maintains each C_{sd} full-rank when merging the symbols.

Algorithm 5: Variable Initialization

1: **for** each destination $d \in D$ **do**
2: Assign a distinct unit content vector of dimension $|\mathcal{M}_s^D|$ for each MPS.
3: Let P_v be the set of paths going through node v in all the MPSs.
4: Let $\mathcal{P}$ be the set of all non-empty P_v, $v \notin D$.
5: Let P_{sd} be the set of the paths from s to d.
6: Setup basis matrices C_{sd}.
7: **end for**
8: **for** each path p **do**
9: Setup content vectors c_p to be the same as the content vector of the corresponding MPS.
10: Setup information carrying FI $i_p \leftarrow p$.
11: Setup node pointers $n_p \leftarrow s$.
12: **end for**

Algorithm 6: Cycle-aware coding algorithm

Input: The set of MPSs $\mathcal{M}_s^D$ with the source s and the set of destinations D.
Output: The codecs at each node v traversed by some path in $\mathcal{M}_s^D$.

1: Initialize the variables (Algorithm 5).
2: **while** $\mathcal{P} \neq \emptyset$ **do**
3: Obtain the next node v to code by Algorithm 4
4: Generate the codecs at v by Algorithm 3.
5: $\mathcal{P} \leftarrow \mathcal{P} \setminus P_v$.
6: **end while**
7: **for** $d \in D$ **do**
8: Let $P_{sd} = \{p_1, p_2, \ldots, p_n\}$. Register at destination d a decoding code map

$$\text{mapping: } (i_{p_1}, i_{p_2}, \ldots, i_{p_n}) \rightarrow (p_1, p_2, \ldots, p_n),$$
$$\text{code matrix: } C_{sd}^{-1}.$$

9: **end for**

CHAPTER 6

IMPLEMENTATION CHALLENGES

In this chapter, we describe the implementation challenges of our system design. We categorize the main challenges into four major groups: load balancing, codec efficiency, coding performance, and memory management. In the following subsections, we describe those challenges and the corresponding methods CodedBulk adopt to deal with them.

6.1 Load Balancing

Since a network is shared by a huge number of flows, the bandwidth available for each flow is usually asymmetric. We elaborate below the load balancing techniques in CodedBulk.

6.1.1 Hop-by-Hop Data Accumulation

In CodedBulk, we adopt hop-by-hop TCP to send coded traffic as stated in Section 4.3. Without any rate control mechanism, greedy hop-by-hop transfer can result in data accumulation at the intermediate nodes when the incoming rate is larger than the outgoing rate. Such accumulation can be unbounded when the downstream links are shared and congested while there is plenty of bandwidth on the upstream links.

To avoid unbounded accumulation, one can perform rate control over the hop-by-hop TCPs. In CodedBulk, we utilize a back-pressure based rate control

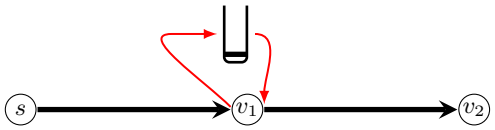

(a) The coded traffic fully utilizes all available bandwidth.

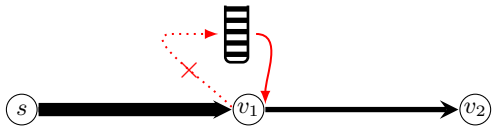

(b) A full buffer will stop taking input from the receiver.

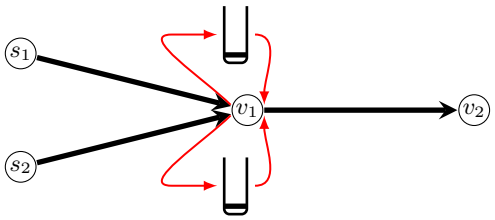

(c) Two buffers are installed per TCP receiver when multiple inputs are merged into one output.

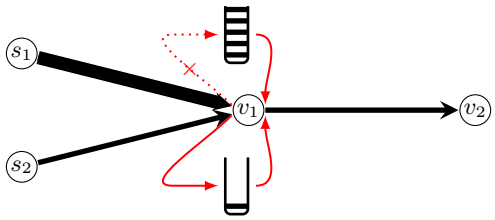

(d) As such, the sending rates of the upstream TCPs are both confined by the downstream.

Figure 6.1: The imbalanced bandwidth between the upstream and the downstream TCPs is handled by a back-pressure rate control mechanism using buffers. One buffer is associated with each TCP receiver. Once the upstream TCP sends faster than the downstream. The buffer will be filled and stop getting input, which slows down the upstream TCP.

as shown in Figure 6.1 that can be done locally. The idea is simple: we introduce an RX buffer at the proxy for each FI^r and impose a limit on it. Such a proxy RX buffer keeps pulling data from FI^r until it is full. When the proxy RX buffer is full and stops pulling from FI^r, the TCP RX buffer of FI^r will be filled and the transport layer protocol slows down FI^r automatically. Meanwhile, an input symbol is removed from the proxy RX buffer when its corresponding output symbols are sent. As such, the downstream congestion can slow down the upstream by this simple design.

6.1.2 Concurrent Multicast Flows

An inter-datacenter network may carry multiple concurrent multicast flows. Supporting multiple flows can easily be done with CodedBulk by superposition. As long as a distinct FI is given to each path, the codecs generated for each multicast flow will access different FI^rs and FI^ts.

Distinct FIs allow multiple multicast flows send through the network at the same time. What is left unspecified is the bandwidth sharing amongst the concurrent bulk traffic. In CodedBulk, we leverage the underlying TCP congestion control mechanism to lead to the fair-share convergence of the hop-by-hop TCP connections. Together with the rate control design in Section 6.1.1, the bandwidth sharing at each link can be automatically achieved.

6.1.3 Asymmetric Bandwidth and Blocking Effect

Although Algorithm 6 does not need the bandwidth information for each path to generate the codecs, asymmetric available bandwidth can still affect the performance of coding. We illustrate the problem below.

Consider a codec which merges two data streams from ${p_1}^r$ and ${p_2}^r$ to one output data stream. If the data rate of ${p_1}^r$ is smaller than ${p_2}^r$, the codec can only output at the data rate no more than ${p_1}^r$'s. As a result, the unprocessed ${p_2}^r$ data is accumulated. Given the back pressure rate control mechanism in Section 6.1.1, ${p_2}^r$ will reduce its data rate when the accumulation exceeds the imposed limit. In other words, the low data rate of ${p_1}^r$ "blocks" ${p_2}^r$, and hence we name this phenomenon the *blocking effect*.

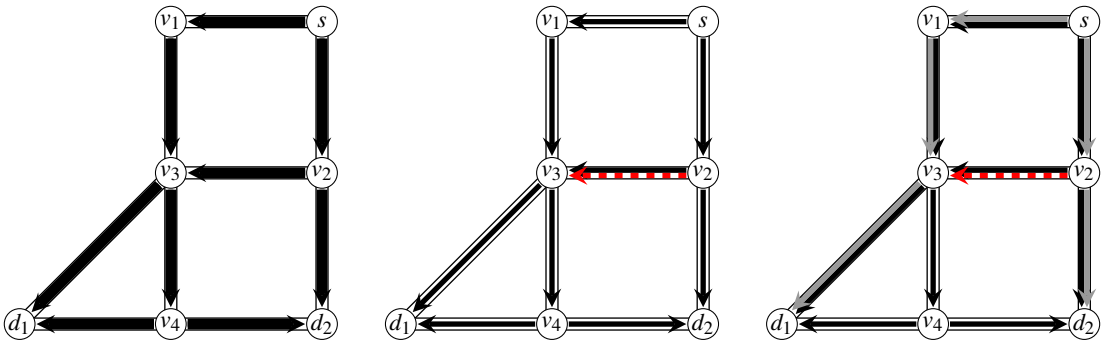

(a) The coded traffic fully utilizes all available bandwidth.

(b) Sharing bandwidth with other traffic leads to bandwidth under-utilization.

(c) We can still send non-coded traffic to the destinations.

Figure 6.2: The blocking effect at v_3 downgrades the coded throughput. Coded-Bulk prioritizes coded traffic over non-coded traffic to mitigate the performance degradation caused by the blocking effect.

Blocking effect happens when the available bandwidth is asymmetric for the incoming FI^{r}s. Such asymmetry can result from the difference in the link capacity or the existence of the sharing traffic. In Figure 6.2, we demonstrate the blocking effect using the 7-node example.

The coded traffic in Figure 6.2(a) can fully utilize all the available bandwidth when no other traffic is present. Suppose some interactive traffic, marked as the dashed arrow, goes through the edge (v_2, v_3), the coded traffic that can be sent through the edge reduces. Accordingly, the blocking effect occurs at v_3 when the codecs merge the traffic (based on the code maps in Table 4.1), which leads to cascade throughput deduction and the bandwidth under-utilization at each edge as in Figure 6.2(b).

Although no more coded traffic can be pushed into the network when blocking effect happens, we can still make the best use of the residual bandwidth by pumping non-coded traffic into network. As shown in Figure 6.2(c), we can still send non-coded traffic through the paths p_1 and p_3 in Figure 4.5(a) to the des-

tinations. CodedBulk adopts a prioritization approach to prefer sending coded traffic over non-coded traffic. As such, CodedBulk codes as much traffic as possible, while filling the unused bandwidth under the blocking effect by the non-coded traffic.

6.2 Codec Efficiency

At each node, the same coding function can be performed using different combinations of codecs. These combinations may be equivalent in theory, while the efficiency can differ in practice due to asymmetric output bandwidth and network asynchrony. In this subsection, we illustrate two such situations and our codec assignment techniques to improve the coding efficiency.

6.2.1 Code Map Decoupling

A multi-row code map describes a codec that outputs to several FI$'$s at the same time. It works fine when none of the FI$'$s encounters congestion. Once one of the FI$'$s congests, the codec gets stuck although other FI$'$s might still have enough bandwidth.

One way to deal with the issue is to divide the codec to a set of codecs, each of which outputs to one FI$'$ only. It can be done by decoupling the multi-row code matrix into several code maps consisting of single-row matrices. For

instance, a code map

$$\text{mapping: } (p_1, p_2) \rightarrow (p_1, p_2),$$
$$\text{code matrix: } \begin{bmatrix} 1 & 2 \\ 2 & 1 \end{bmatrix}$$

can be decoupled into two code maps

$$\text{mapping: } (p_1, p_2) \rightarrow (p_1), \qquad \text{and} \qquad (p_1, p_2) \rightarrow (p_2),$$
$$\text{code matrix: } \begin{bmatrix} 1 & 2 \end{bmatrix}, \qquad \begin{bmatrix} 2 & 1 \end{bmatrix}.$$

Such decoupling not only avoids the asymmetric output bandwidth issues but also allows parallel computation.

6.2.2 Redundant Dependency Reduction

To merge several data streams, a codec waits for the receipt of all streamed input symbols before merging. Since the network is asynchronous, the arrival of the input symbols varies in time, which degrades the coding efficiency.

In some cases, the efficiency degradation can be mitigated by expecting fewer input streams. One such cases is when redundancy exists in the code map. More specifically, the column dimension of a single-row code matrix can be reduced without changing the output of the corresponding code map if some zero entries exist. For instance, the code map

$$\text{mapping: } (p_1, p_2, p_3) \rightarrow (p_1),$$
$$\text{code matrix: } \begin{bmatrix} 1 & 0 & 2 \end{bmatrix}$$

is equivalent to

$$\text{mapping: } (p_1, p_3) \rightarrow (p_1),$$
$$\text{code matrix: } \begin{bmatrix} 1 & 2 \end{bmatrix}.$$

Eliminating the zero entries reduces the number of input data streams the codec needs to wait, which mitigates the impact of network asynchrony.

6.3 Coding Performance

To achieve high coding throughput, the proxy should perform the computation efficiently. We introduce the following performance improvement techniques to accelerate coding process.

6.3.1 Simple Forwarding

Coding is in general an expensive operation as it involves per-symbol arithmetic operations. A simple idea to improve the coding performance is then to avoid as many arithmetic operations as possible. In fact, there exists a special case in which coding can be performed without any arithmetic operation: forwarding.

As shown in Example 4.5.1, a forwarding code map consists of an identity coding matrix. The codec can perform coding by simply bypassing the data streams from the FI^rs to the corresponding FI^ts. In practice, such bypassing can be done much more efficiently than the per-symbol identity multiplication. In CodedBulk, forwarding involves only passing the memory pointers.

6.3.2 Batch Processing

With code maps, coding the symbols of the incoming data streams is a simple code matrix multiplication. Such operation can be done when the input symbols are in place. Since the incoming data streams are asynchronous, it is possible that some input symbols of a codec are received earlier than the others, and the codec will need to wait until all the symbols arrive.

Due to the asynchronous nature of the incoming data streams, a codec performing per-symbol coding is forced to switch between the waiting phase and the coding phase, which is highly inefficient as several function calls may be involved. A better way to handle the asynchrony is to perform batch coding, i.e., collecting more symbols and coding them together.

We design *tasks* for this purpose. Each task waits for a certain block of symbols. Once the blocks are received from all input streams, the task will be processed.

To denote the block of symbols, we receive and save data streams in blocks and mark each block a *serial number*. As a task collects the inputs with, and marks the outputs by, the same serial number, we can also refer to a task by its codec and the serial number of the blocks it waits for.

As an example, consider a codec taking three data streams corresponding to FI p_1, p_2, and p_3 as the inputs in Figure 6.3. Blocks are created by packing every 10 received symbols (shaded symbols) and we assign each block a serial number in order. Whenever a new serial number is assigned, we create a corresponding task. In the example, three tasks are created, and task 1 has collected all the blocks to be coded.

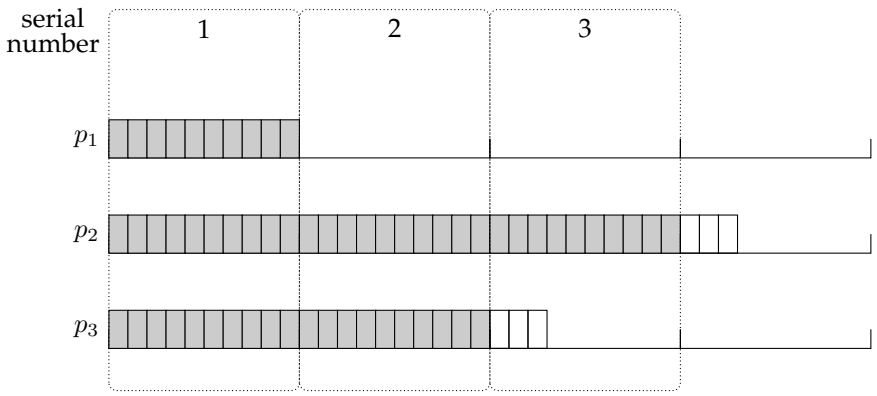

Figure 6.3: Three tasks in a codec, represented by the dotted rectangles, take p_1, p_2, and p_3 as the inputs. Each small rectangle represents a symbol. In this example, 10 symbols form a block (shaded symbols), and task 1 is ready to be coded.

A task that has collected all blocks is called a *ready task* and moved to a *ready task queue* for coding. The processor will pull tasks from the ready task queue and generate the outputs accordingly. Instead of pulling one task at a time, the processor will pull a batch of them whenever it is possible. Such batch processing mitigates the contention of accessing the ready task queue where ready tasks are enqueued and the processor dequeues tasks.

6.3.3 Parallel Computing and In-order Delivery

Parallel computing is a common technique to boost the throughput of a system. We illustrate below the task-level parallelism in CodedBulk, while hardware-aid symbol-level parallelism is also possible as stated later.

In CodedBulk, we implement a *thread pool* that maintains a set of *worker threads*. Each worker thread pulls and codes a batch of tasks from the ready task queue. The architecture is shown in Figure 6.4.

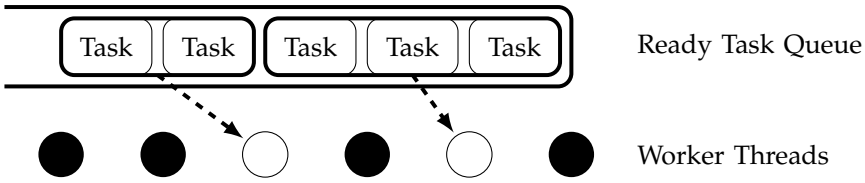

Figure 6.4: A thread pool consisting of 6 worker threads performs coding. Each filled circle is a running thread, while an empty circle represents an idle thread. Each idle thread pulls a batch of tasks from the ready task queue and starts coding.

It is noticeable that coding a task can be accelerated by hardware. Essentially, a task is a collection of several per-symbol arithmetic operations. With the aid of hardware, these operation can be parallelized to boost the throughput.

Although parallelism and batch processing boost the coding throughput, they disturb the order of the data streams. Since the proxies run at the application layer, we have to restore the order before releasing the disturbed output data stream. Using the serial numbers, we sort the blocks of output symbols to restore in-order delivery.

6.4 Memory Management

We adopt the store-and-forward model to merge the incoming data streams, which requires memories for storing the incoming data. Although the allocation of the memories can be handled by the underlying operating system, we manually acquire, manage, and release the memory to improve the coding performance. The advantage is significant: as shown in Figure 6.5, manual memory management leads to around twice the throughput than relying on the operating system when we increase the number of worker threads. We describe below

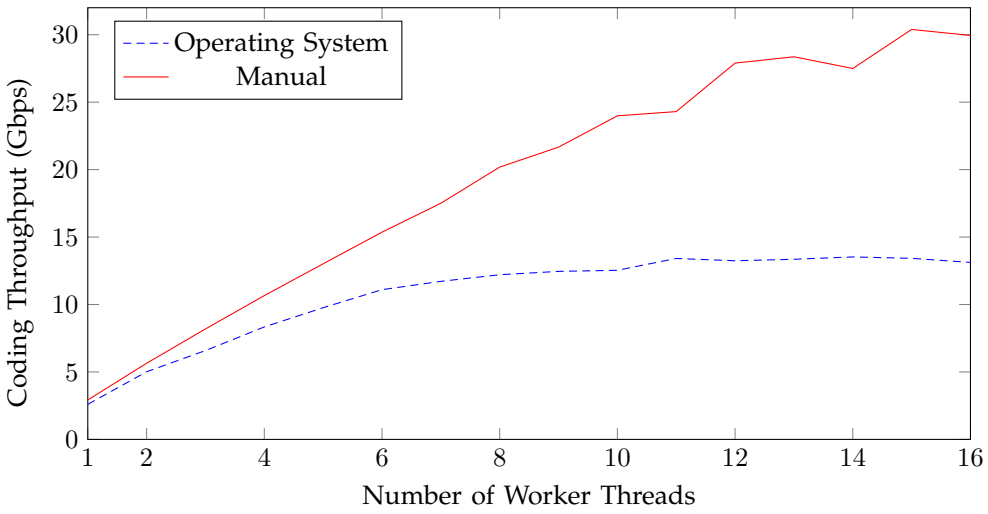

Figure 6.5: The comparison of the coding throughput under operating system and manual memory management. On a 16-core server, increasing the number of worker threads gives nearly linear throughput gain when managing memory manually. Operating system, however, cannot fully enjoy the additional computation resources.

our memory management techniques.

6.4.1 Local Memory Allocation

The reason that the operating system fails to achieve high coding throughput in Figure 6.5 is the frequent memory allocation/deallocation. Such memory acquisition operations are time consuming and eventually block the computation when storing the coded output symbols. To prevent doing so, we ask for a sufficiently large chunk of memory from the operating system upon the establishment of an FI^r and the creation of a worker thread. We then locally store the incoming data streams at the receiving FI^r and the outgoing coded symbols at the producing worker thread. With an appropriate flagging system over the original memory chunk, we achieve high performance memory allocation/deallocation with flags.

6.4.2 Notifier and Memory Deallocation

As demonstrated in Table 4.1 and Section 6.2.1, an input data stream may be merged by the codecs to produce different output data streams. Since each FI^t may stream in distinct data rate and we perform the input rate control by buffer limitation as stated in Section 6.1.1, we should release a stored input symbol after all its corresponding output symbols are generated and sent. To do so, we maintain a counter for each input block and introduce a *notifier* for each task.

When a serial number is assigned to an input block, its counter is set to keep track of the total number of tasks that depend on the input block. Meanwhile, each notifier at a task maintains a counter that tracks the number of unsent outputs coded from the task. While all the outputs are sent, the notifier deallocates the memory of the task and decrements the corresponding input block counters. Similarly, when the input block counter returns to zero, the memory of the input block is released.

Together, the input block counters and the notifiers guarantee the memory deallocation of an input block after all dependent output symbols are sent.

CHAPTER 7

EVALUATION

In this chapter, we evaluate the performance of CodedBulk through extensive experiments. The chapter starts with our experimental setup and performance metric in Section 7.1. We first showcase the performance of CodedBulk via inter-datacenter WAN experiments in Section 7.2. In comparison with the inter-datacenter WAN experiments that run in the wild, we conduct experiments over our fully controlled testbed in Section 7.3. Finally, Section 7.4 demonstrates the scalability of CodedBulk by software-based and hardware-based microbenchmarks.

7.1 Setup

We elaborate our experimental setup below. Starting with the evaluated scenarios and the performance metrics, we then describe the network settings and the traffic workloads behind the scenes.

Evaluated Scenarios We consider three bulk transfer scenarios for comparison: unipath multicast, multipath multicast, and CodedBulk. These three scenarios are different in the way the bulk traffic is sent. In the unipath multicast scenario, the bulk traffic is sent from the source to each destination using a single chosen multicast path set. For evaluation, we consider the path set obtained by shortest paths from source to each destination. The second scenario is when the network is allowed to send bulk traffic via all available multicast path sets, but not employing network coding. We employ TCP fair sharing for this scenario

to distribute bandwidth among various multicast path sets. The CodedBulk scenario is our network coded bulk transfer design.

Besides the three bulk transfer scenarios, we also calculate the ideal throughput for the controlled testbed. The ideal scenario gives the ideal CodedBulk steady state performance assuming that hop-by-hop TCPs acquire their fair sharing bandwidth. Under the ideal setting, the header overhead is considered (40 bytes per 1500 byte packet) while the transient behaviors, such as additive-increase-multiplicative-decrease and delay, are ignored.

Performance Metric The key performance metric used to adjudge CodedBulk's benefits is the *normalized aggregate throughput* (NAT). NAT is calculated by normalizing the aggregate throughput by the link capacity. We obtain the aggregate throughput of both bulk and interactive traffic by aggregating the throughput of the corresponding transfers. The throughput of a transfer is the average of the measured throughput, in data rate, at each destination. For example, the throughput of a unicast transfer is simply the receiving data rate at its destination, while the throughput of a multicast transfer with two destinations is the summation of the receiving data rates at both destinations divided by two.

Network Settings Our experiments are conducted based on three network topologies: the 7-node example (Figure 3.2), B4 (Figure 3.1), and Internet2 (Figure 7.1), where Internet2 [47] and B4 are already employed WAN topologies, and the 7-node example is a subset of B4.

We establish the topologies under two different experiment environments:

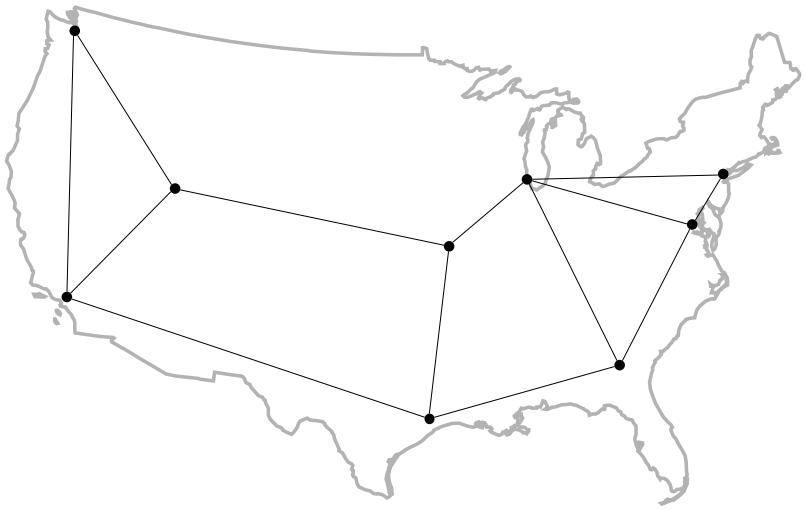

Figure 7.1: The topology of Internet2 network, a high-speed wide-area network established for research and education.

inter-datacenter WAN and controlled testbed. The inter-datacenter WAN environment incorporates real world impacts on the performance of CodedBulk such as cross-continental propagation delay and varying link bandwidth, while the controlled testbed does not reflect those factors.

Under the inter-datacenter WAN environment, we replicate B4 and Internet2 topologies on Amazon EC2 by launching geographically distributed server instances among various cluster regions. The locations of the servers are selected to match the target topology as closely as possible. Each link within the target topology is emulated by a pair of network interface cards (NICs), whose available bandwidth is throttled by the link capacity. Accordingly, the traffic going through a link is sent between its corresponding pair of NICs and routed by underlying routing mechanisms.

On the other hand, we establish our controlled testbed on a simple star-shaped network with an OpenFlow switch at the hub. The testbed emulates a target topology by representing each node in the topology by a server at the

leaves. A link between a pair of data centers is emulated by a fixed path through the hub provided by the network layer between the corresponding servers. Again, we throttle the bandwidth of the path to provide the designated link capacity.

Workloads The network is loaded with randomly generated low-priority bulk and high-priority interactive traffic. Each bulk transfer is a multicast session from a source to several chosen destinations; while each interactive transfer is a unicast session between a source-destination pair. All the traffic source pushes data into the network whenever the available bandwidth allows. A bulk source has infinite amount of data to send. On contrary, an interactive source disseminates time-dependent workload.

We generate traffic as follows. A number of nodes are randomly selected as the bulk traffic sources and each bulk session is associated with a number of random destinations. On the other hand, interactive traffic is generated for specific network load levels (mainly around 5 to 20% of network capacity) and the loading level 0% refers to the case without interactive traffic. Given a load level, we generate the data transferred across the network by constructing a series of randomly sampled source, destination, arrival time, and data size. Among the generated data transfers, we bundle those with the same source/destination pair as one interactive transfer for the purpose of congestion control.

In the following experiments, we impose a baseline case consisting of 6 bulk transfers multicasting to 4 destinations each. Without further specification, no interactive traffic is considered in the baseline case.

7.2 Inter-Datacenter WAN Experiments

We first demonstrate the effectiveness of CodedBulk under the inter-datacetner WAN environment. Figure 7.2(a) and Figure 7.2(b) show the NAT of bulk and interactive traffic for the three aforementioned scenarios – unipath, multipath, and coded multicast (CodedBulk) – under B4 and Internet2 topologies.

As shown in the figures, none of the scenarios changes the interactive traffic throughput since it is assigned the highest priority. In contrast, CodedBulk increases the bulk throughput over the unipath multicast by around 2.6 times for B4 and 1.9 times for Internet2. Multicasting through multiple path sets grants more throughput improvement over unipath mutlicasting on B4 comparing to Internet2. The reason is that B4 has higher path diversity, i.e., it is less likely to have overlapped paths. As a result, load balancing among multiple path sets helps. On the other hand, multipath also introduces connection overhead. When the load balancing gain is not enough to compensate the connection overhead, the throughput performance can degrade as we see in Figure 7.2(b). In both figures, increasing the loading level of interactive traffic reduces the lower priority bulk traffic, but the improvements of CodedBulk over other two scenarios remain almost constant independent of interactive traffic load.

7.3 Controlled Testbed Experiments

We then examine the performance of CodedBulk on our controlled testbed, which emulates B4 and Internet2 topologies. Figure 7.3 shows NAT for bulk and interactive traffic for the baseline workload with varying interactive traffic

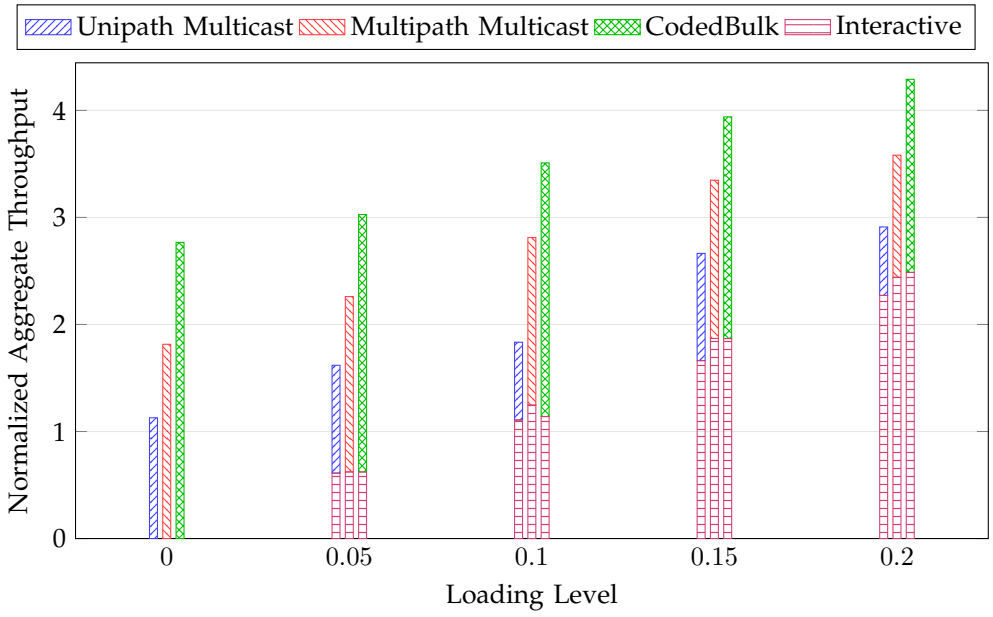

(a) B4

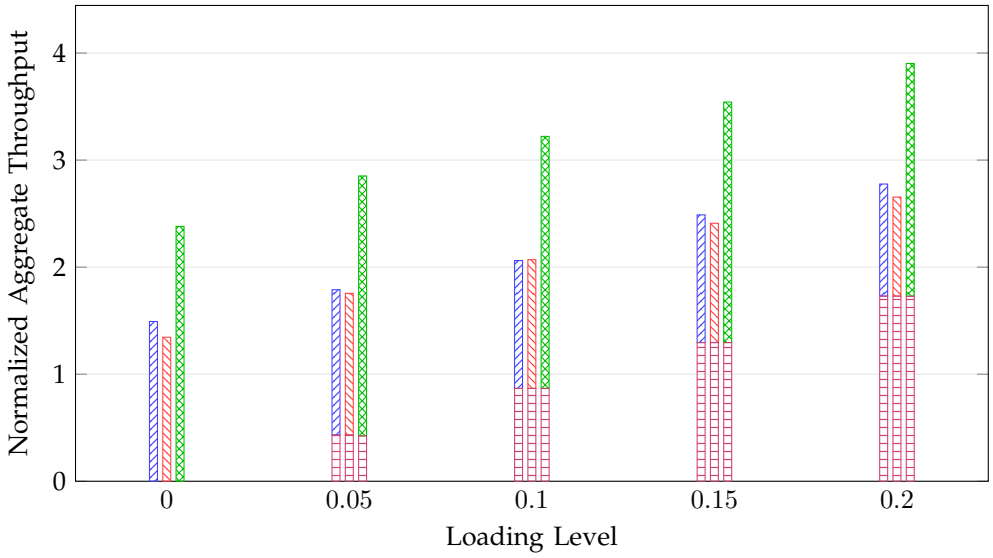

(b) Internet2

Figure 7.2: We conduct inter-datacenter WAN experiments on Amazon EC2 based on replicated topologies according to the well-known WANs B4 and Internet2. In each experiment, 6 distinct bulk sessions, each multicasts to 4 destinations, are scheduled by CodedBulk along with various loading levels of high-priority interactive traffic. Under both B4 and Internet2 topologies, the results show that CodedBulk improves the bulk throughput by 1.5 to 3 times. The relative improvement stays nearly the same when the interactive traffic grabs more bandwidth from the bulk traffic under higher loading levels.

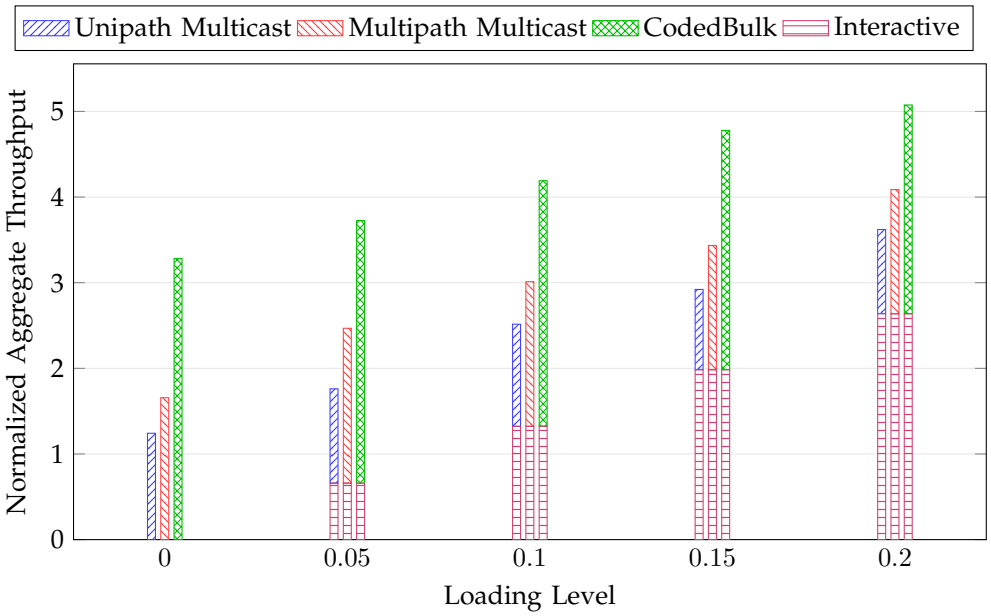

(a) B4

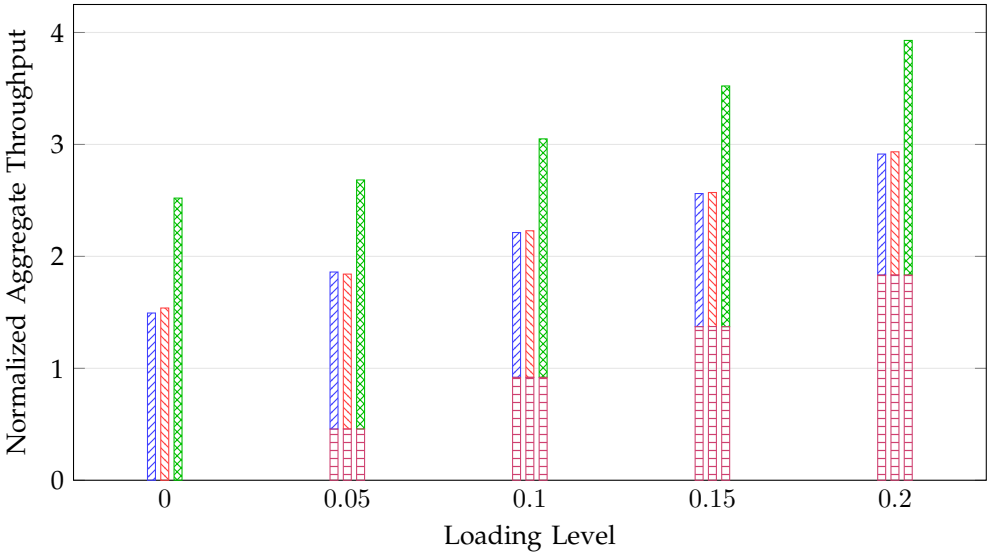

(b) Internet2

Figure 7.3: Using our controlled testbed, we emulate B4 and Internet2 topologies to compare the performance of CodedBulk under the baseline scenario (6 bulk source, each has 4 destinations) with different interactive traffic loading levels. The trend of the results match the WAN experiments', while the performance gain is higher.

load. As expected, Figure 7.3(a) and 7.3(b) both show similar trends in performance gains as in Figure 7.2(a) and 7.2(b) respectively. The absolute value of NAT is higher in the controlled testbed, since the RTT in the testbed is shorter comparing to WAN and there is no other co-existing traffic that might interfere the performance.

We also run several experiments to showcase the effect of varying number of bulk transfers and number of destinations per transfer on the CodedBulk performance benefits.

Varying Number of Bulk Transfers Figure 7.4(a) and 7.4(b) shows CodedBulk performance gains for varying number of concurrent bulk transfers. Each transfer has 4 randomly chosen destinations. The NAT increases when more concurrent bulk sessions exist and it saturates in the meantime due to the fixed available link capacity. Although the blocking effect among bulk sessions causes the relative throughput gain decreases from around 2 to 4 times, the gain is still significant. Also, the average of the ideal throughput shows that the CodedBulk achieves the throughput close to the ideal.

Varying Number of Destinations per Transfer Figure 7.5(a) and 7.5(b) showcases NAT for the case with 6 concurrent bulk transfers but varying number of destinations per transfer. Increasing the number of destinations for a fixed number of bulk transfer would decrease the aggregate throughput as more network resources would be spent on each transfer. However, more destinations also create more room for network coding to improve the performance. In theory, a well-coded bulk transfer will be able to achieve min-cut throughput per destination. Although bandwidth sharing among different multicast session

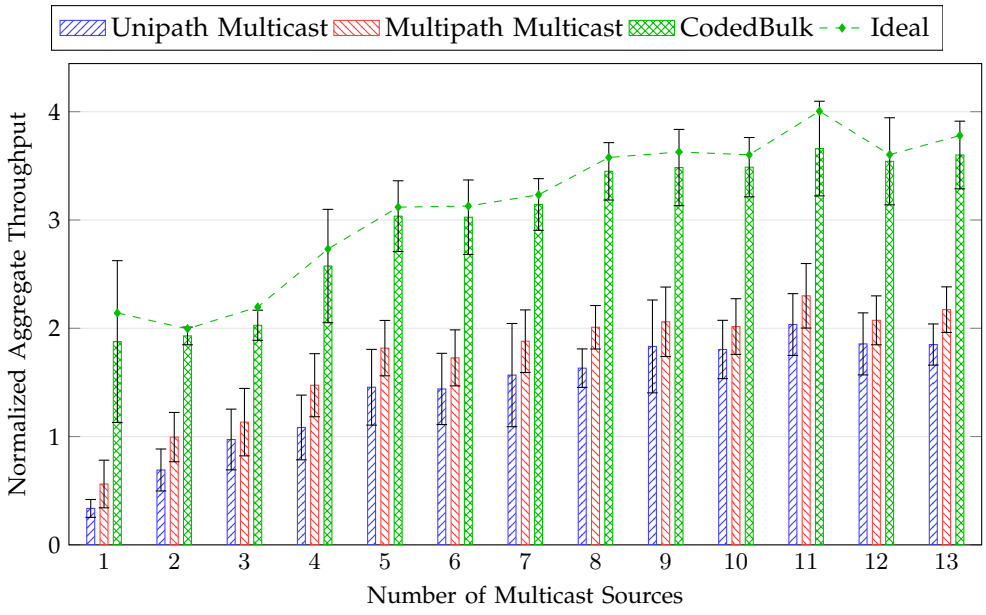

(a) B4

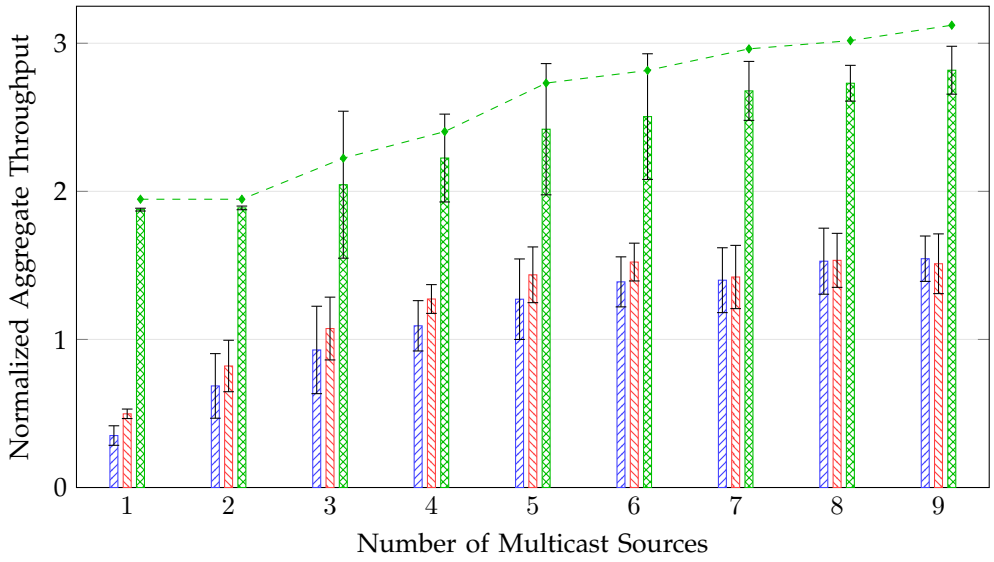

(b) Internet2

Figure 7.4: In the controlled testbed emulating B4 and Internet2, we randomly generate different number of sources multicasting to 4 random destinations each. The aggregate throughput increases as more bulk traffic is created. The average throughput of the ideal scenarios is also plotted, which suggests that the results are close to the ideal scenarios.

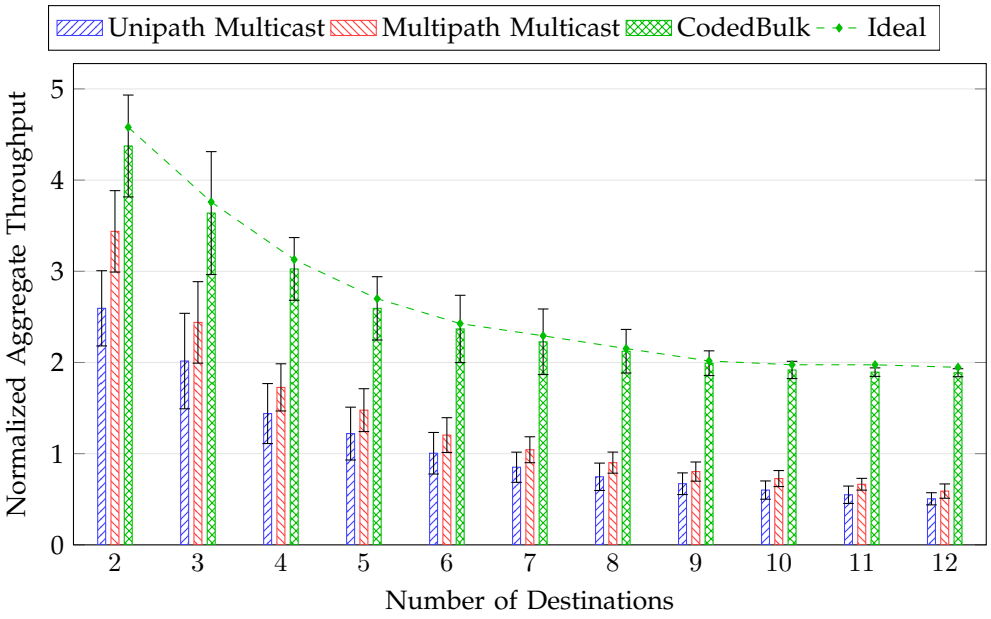

(a) B4

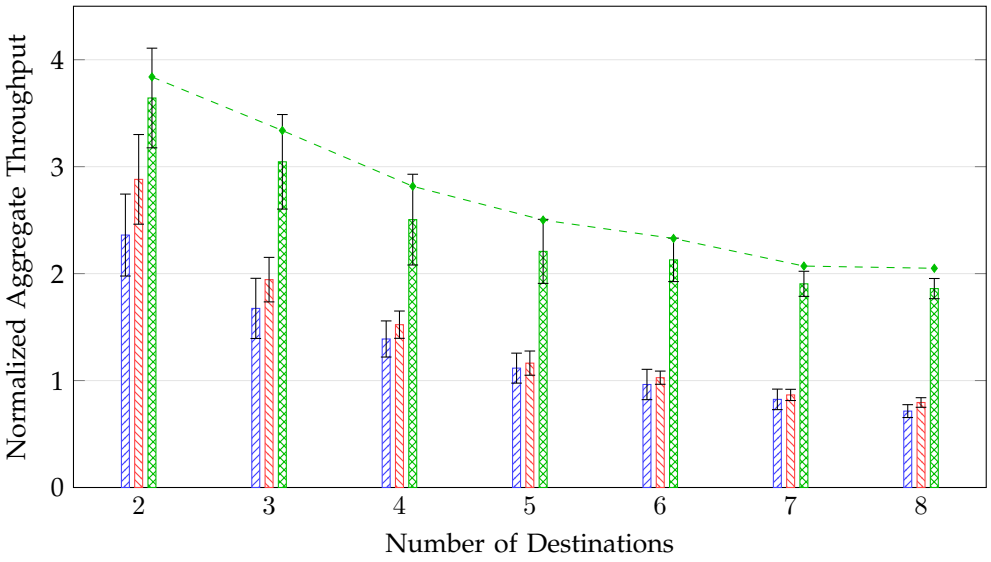

(b) Internet2

Figure 7.5: 6 concurrent bulk transfers multicast to various number of destinations in the controlled testbed emulating B4 and Internet2. As each bulk session sends to more destinations, the bandwidth sharing leads to throughput degradation. However, CodedBulk improves the relative gain in the presence of more destinations. The results are close to the ideal throughput.

induces the blocking effect that diminishes such coding benefit, we can still observe the improvement of the relative performance gain when more destinations are added. Similarly, our results are close to the ideal.

7.4 Microbenchmarks

We also conduct several experiments to determine the scalaibility of CodedBulk through software and hardware microbenchmarks.

7.4.1 Software implementation

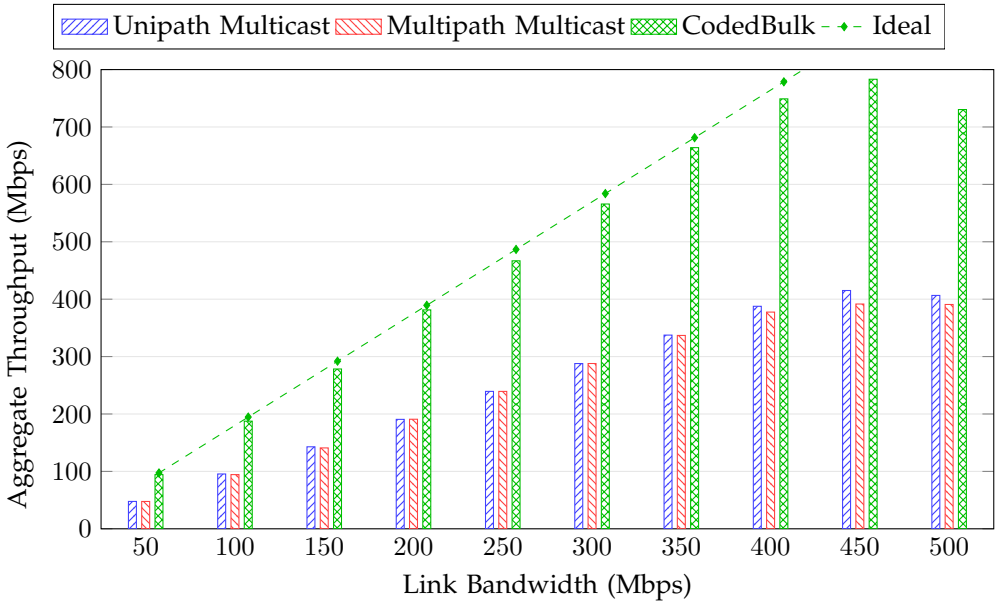

Figure 7.6: We evaluate the scalability of the system by deploying the 7-node example on our controlled testbed. Under varying access link capacity, the performance of CodedBulk is sustained when enough resources are available up to around 450 Mbps. Before then, CodedBulk can achieve the throughput almost identical to the ideal throughput.

Since CodedBulk requires computation at each node for performing cod-

Element	Used	Available	Utilization
LUT	736	433200	0.17%
BRAM	16.5	1470	1.12%

Table 7.1: Resource utilization of a 128-bit codec using Xilinx Virtex-7 XC7VX690T FPGA. Our implementation can provide up to 31.25 Gbps throughput with 0.17% LUTs and1.12% BRAMs. No DSP is needed in our design.

ing/decoding operations, for a fixed compute capacity, the performance gains should start to debilitate after increasing link bandwidths at a certain threshold amount because of scarce computation power, memory, or link bandwidth. When the resources are sufficient, we would expect the throughput gain proportional to the bandwidth increase. We try to obtain that threshold link capacity for the 7-node topology using 4-core servers with modest 4 GB RAM and a NIC of 1 Gbps access link capacity emulating the incoming/outgoing network interfaces. The results are shown in Figure 7.6, which suggest the threshold link capacity is around 450 Mbps. Before reaching 450 Mbps, the aggregate throughput scales linearly as expected, and it is almost identical to the ideal throughput. The reason of the performance degradation at 450 Mbps is due to the lack of emulated link bandwidth and computational resources. Given the linear growth under sufficient resources, the system would keep scaling linearly and the threshold link capacity would be pushed upward when sufficient resources are supplied.

7.4.2 Hardware implementation

Inter-DC links are usually of several hundred Gbps bandwidths, and pure software computation can be the bottleneck to support such a high throughput. To

tackle this issue, we leverage hardware to parallelize the computation and provide line-rate coding.

We synthesize a simple 128-bit codec that can process 16 symbols (bytes) within one clock cycle on Xilinx Virtex-7 XC7VX690T FPGA, which offers 100, 200, and 250 MHz fabric clocks. With respect to the clocks, our FPGA-based codec can achieve throughput 12.5, 25, and 31.25 Gbps. Without needing any DSP, our hardware design consumes only 0.17% LUTs and 1.12% BRAMs as shown in Table 7.1, and hence it can be scaled easily to provide even higher throughput.

CHAPTER 8

SUMMARY AND FUTURE WORK

This chapter summarizes the achievements of CodedBulk and portrays the possible next steps and the future extensions of the work.

8.1 Current Achievement

In this dissertation, we design and implement CodedBulk to improve the throughput of inter-datacenter bulk transfers using network coding. Our approach is possible thanks to the new properties exhibited by the inter-datacenter context, including delay-tolerant bulk transfers, small-scale programmable networks, and resource-rich intermediate nodes. We leverage those design opportunities to overcome the implementation challenges. Through the inter-datacenter experiments, the resulting CodedBulk demonstrates a twice to four times throughput improvement of the inter-datacenter bulk traffic.

8.2 Possible Improvement

Close-loop control over coding schemes CodedBulk operates under an open-loop control: Given the multicast sessions reported from the multicast agent senders, the controller computes and deploys the coding scheme to the network based on its current global view. However, the varying interactive traffic leads to different topology for the bulk traffic, which can impact the effectiveness of the deployed coding schemes. This issue can be alleviated if the centralized

controller reevaluates the installed coding scheme once a while based on the updated global view. That gives a feedback-style close-loop control.

Localized coding The generation of coding schemes depends on a global view from one centralized controller, which prevents a full distributed computation and exposes the system under a single point of failure. By extending the code generation algorithm to compute based on only the localized information, the information that is collected from only a part of the network, we would be able to distribute the computation to several controllers and improve the robustness of the system.

8.3 Future Directions

Time-dependent coding Although our cycle-aware coding algorithm can deal with cyclic network topology, our approach does not guarantee the min-cut throughput per destination even in theory. One way to achieve the optimal coding throughput in a cyclic network is through the time-dependent convolutional network coding. Convolutional network coding requires coding the symbols sent out from the source at different time. To support convolutional network coding, we will need to extend our code map and algorithm designs.

Learning-based coding Recently, machine learning has demonstrated its great potential in making predictions and dealing with non-linear optimization. As such, an online feedback system can adopt machine learning as its controller and improve the dynamic performance. Is might be possible to use machine

learning to monitor the incoming interactive traffic and update the codecs on the fly.

BIBLIOGRAPHY

[1] Mohammad Al-Fares, Alexander Loukissas, and Amin Vahdat. A scalable, commodity data center network architecture. *ACM SIGCOMM CCR*, 38(4):63–74, 2008.

[2] Arjun Roy, Hongyi Zeng, Jasmeet Bagga, George Porter, and Alex C Snoeren. Inside the social network's (datacenter) network. *ACM SIGCOMM CCR*, 45(4):123–137, 2015.

[3] Arjun Singh, Joon Ong, Amit Agarwal, Glen Anderson, Ashby Armistead, Roy Bannon, Seb Boving, Gaurav Desai, Bob Felderman, Paulie Germano, et al. Jupiter rising: A decade of Clos topologies and centralized control in Google's datacenter network. *ACM SIGCOMM CCR*, 45(4):183–197, 2015.

[4] Yu Wu, Zhizhong Zhang, Chuan Wu, Chuanxiong Guo, Zongpeng Li, and Francis CM Lau. Orchestrating bulk data transfers across geo-distributed datacenters. *IEEE Trans. Cloud Comput.*, 5(1):112–125, 2017.

[5] Chunqiang Tang, Thawan Kooburat, Pradeep Venkatachalam, Akshay Chander, Zhe Wen, Aravind Narayanan, Patrick Dowell, and Robert Karl. Holistic configuration management at Facebook. In *Proc. ACM SOSP*, pages 328–343. ACM, 2015.

[6] Sushant Jain, Alok Kumar, Subhasree Mandal, Joon Ong, Leon Poutievski, Arjun Singh, Subbaiah Venkata, Jim Wanderer, Junlan Zhou, Min Zhu, Jonathan Zolla, Urs Hölzle, Stephen Stuart, and Amin Vahdat. B4: Experience with a globally-deployed software defined WAN. *ACM SIGCOMM CCR*, 43(4):3–14, 2013.

[7] Chi-Yao Hong, Srikanth Kandula, Ratul Mahajan, Ming Zhang, Vijay Gill, Mohan Nanduri, and Roger Wattenhofer. Achieving high utilization with software-driven WAN. *ACM SIGCOMM CCR*, 43(4):15–26, 2013.

[8] Andrew Hiles. Five nines: Chasing the dream? `http://www.continuitycentral.com/feature0267.htm`.

[9] Yingying Chen, Sourabh Jain, Vijay Kumar Adhikari, Zhi-Li Zhang, and Kuai Xu. A first look at inter-data center traffic characteristics via Yahoo! datasets. In *Proc. IEEE INFOCOM*, pages 1620–1628. IEEE, 2011.

[10] Nikolaos Laoutaris, Michael Sirivianos, Xiaoyuan Yang, and Pablo Rodriguez. Inter-datacenter bulk transfers with NetStitcher. *ACM SIGCOMM CCR*, 41(4):74–85, 2011.

[11] Rudolf Ahlswede, Ning Cai, Shuo-Yen Robert Li, and Raymond W Yeung. Network information flow. *IEEE Trans. Inf. Theory*, 46(4):1204–1216, 2000.

[12] Shuo-Yen Robert Li, Raymond W Yeung, and Ning Cai. Linear network coding. *IEEE Trans. Inf. Theory*, 49(2):371–381, 2003.

[13] Sharad Agarwal, John Dunagan, Navendu Jain, Stefan Saroiu, Alec Wolman, and Harbinder Bhogan. Volley: Automated data placement for geo-distributed cloud services. In *Proc. USENIX NSDI*, pages 2–2. USENIX Association, 2010.

[14] James C Corbett, Jeffrey Dean, Michael Epstein, Andrew Fikes, Christopher Frost, Jeffrey John Furman, Sanjay Ghemawat, Andrey Gubarev, Christopher Heiser, Peter Hochschild, et al. Spanner: Google's globally distributed database. *ACM TOCS*, 31(3):8, 2013.

[15] Ashish Gupta, Fan Yang, Jason Govig, Adam Kirsch, Kelvin Chan, Kevin Lai, Shuo Wu, Sandeep Govind Dhoot, Abhilash Rajesh Kumar, Ankur Agiwal, Sanjay Bansali, Mingsheng Hong, Jamie Cameron, Masood Siddiqi, David Jones, Jeff Shute, Andrey Gubarev, Shivakumar Venkataraman, and Divyakant Agrawal. Mesa: Geo-replicated, near real-time, scalable data warehousing. *Proc. VLDB Endowment*, 7(12):1259–1270, 2014.

[16] Zhe Wu, Michael Butkiewicz, Dorian Perkins, Ethan Katz-Bassett, and Harsha V Madhyastha. SPANStore: Cost-effective geo-replicated storage spanning multiple cloud services. In *Proc. ACM SOSP*, pages 292–308. ACM, 2013.

[17] Ariel Rabkin, Matvey Arye, Siddhartha Sen, Vivek S Pai, and Michael J Freedman. Aggregation and degradation in JetStream: Streaming analytics in the wide area. In *Proc. USENIX NSDI*, volume 14, pages 275–288, 2014.

[18] Qifan Pu, Ganesh Ananthanarayanan, Peter Bodik, Srikanth Kandula, Aditya Akella, Paramvir Bahl, and Ion Stoica. Low latency geo-distributed data analytics. *ACM SIGCOMM CCR*, 45(4):421–434, 2015.

[19] Ashish Vulimiri, Carlo Curino, Philip Brighten Godfrey, Thomas Jungblut, Jitu Padhye, and George Varghese. Global analytics in the face of bandwidth and regulatory constraints. In *Proc. USENIX NSDI*, volume 7, pages 7–8, 2015.

[20] Nikolaos Laoutaris, Georgios Smaragdakis, Rade Stanojevic, Pablo Rodriguez, and Ravi Sundaram. Delay tolerant bulk data transfers on the Internet. *IEEE/ACM Trans. Netw.*, 21(6):1852–1865, 2013.

[21] Xin Jin, Yiran Li, Da Wei, Siming Li, Jie Gao, Lei Xu, Guangzhi Li, Wei

Xu, and Jennifer Rexford. Optimizing bulk transfers with software-defined optical WAN. In *Proc. ACM SIGCOMM*, pages 87–100. ACM, 2016.

[22] Srikanth Kandula, Ishai Menache, Roy Schwartz, and Spandana Raj Babbula. Calendaring for wide area networks. *ACM SIGCOMM CCR*, 44(4):515–526, 2014.

[23] Hong Zhang, Kai Chen, Wei Bai, Dongsu Han, Chen Tian, Hao Wang, Haibing Guan, and Ming Zhang. Guaranteeing deadlines for inter-data center transfers. *IEEE/ACM Trans. Netw.*, 25(1):579–595, 2017.

[24] John C Lin and Sanjoy Paul. RMTP: A reliable multicast transport protocol. In *Proc. IEEE INFOCOM*, volume 3, pages 1414–1424. IEEE, 1996.

[25] Miguel Castro, Peter Druschel, Anne-Marie Kermarrec, Animesh Nandi, Antony Rowstron, and Atul Singh. SplitStream: high-bandwidth multicast in cooperative environments. In *ACM SIGOPS Operating Systems Review*, volume 37, pages 298–313. ACM, 2003.

[26] Aakash Iyer, Praveen Kumar, and Vijay Mann. Avalanche: Data center multicast using software defined networking. In *IEEE COMSNETS*, pages 1–8. IEEE, 2014.

[27] John Jannotti, David K Gifford, Kirk L Johnson, M Frans Kaashoek, et al. Overcast: Reliable multicasting with an overlay network. In *Proc. USENIX OSDI*, page 14. USENIX Association, 2000.

[28] Mohammad Noormohammadpour, Cauligi S Raghavendra, Srikanth Kandula, and Sriram Rao. QuickCast: Fast and efficient inter-datacenter transfers using forwarding tree cohorts. In *Proc. IEEE INFOCOM*. IEEE, 2018.

[29] Suman Banerjee, Bobby Bhattacharjee, and Christopher Kommareddy. Scalable application layer multicast. *ACM SIGCOMM CCR*, 32(4):205–217, 2002.

[30] Mojtaba Hosseini, Dewan Tanvir Ahmed, Shervin Shirmohammadi, and Nicolas D Georganas. A survey of application-layer multicast protocols. *IEEE Commun. Surveys & Tutorials*, 9(1-4):58–74, 2007.

[31] Ralf Koetter and Muriel Médard. An algebraic approach to network coding. *IEEE/ACM Trans. Netw.*, 11(5):782–795, 2003.

[32] Tracey Ho, Muriel Médard, Ralf Koetter, David R Karger, Michelle Effros, Jun Shi, and Ben Leong. A random linear network coding approach to multicast. *IEEE Trans. Inf. Theory*, 52(10):4413–4430, 2006.

[33] Sidharth Jaggi, Peter Sanders, Philip A Chou, Michelle Effros, Sebastian Egner, Kamal Jain, and Ludo MGM Tolhuizen. Polynomial time algorithms for multicast network code construction. *IEEE Trans. Inf. Theory*, 51(6):1973–1982, 2005.

[34] Philip A Chou, Yunnan Wu, and Kamal Jain. Practical network coding. In *Proc. Allerton*, volume 41, pages 40–49, 2003.

[35] Sachin Katti, Hariharan Rahul, Wenjun Hu, Dina Katabi, Muriel Médard, and Jon Crowcroft. XORs in the air: Practical wireless network coding. *ACM SIGCOMM CCR*, 36(4):243–254, 2006.

[36] Sachin Katti, Shyamnath Gollakota, and Dina Katabi. Embracing wireless interference: Analog network coding. *ACM SIGCOMM CCR*, 37(4):397–408, 2007.

[37] Jonas Hansen, Daniel E Lucani, Jeppe Krigslund, Muriel Médard, and Frank HP Fitzek. Network coded software defined networking: Enabling 5G transmission and storage networks. *IEEE Commun. Mag.*, 53(9):100–107, 2015.

[38] Jay Kumar Sundararajan, Devavrat Shah, Muriel Médard, Michael Mitzenmacher, and Joao Barros. Network coding meets TCP. In *Proc. IEEE INFOCOM*, pages 280–288. IEEE, 2009.

[39] MinJi Kim, Jason Cloud, Ali ParandehGheibi, Leonardo Urbina, Kerim Fouli, Douglas Leith, and Muriel Médard. Network coded TCP (CTCP). *arXiv preprint arXiv:1212.2291*, 2012.

[40] Christos Gkantsidis and Pablo Rodriguez Rodriguez. Network coding for large scale content distribution. In *Proc. IEEE INFOCOM*, volume 4, pages 2235–2245. IEEE, 2005.

[41] Alexandros G Dimakis, P Brighten Godfrey, Yunnan Wu, Martin J Wainwright, and Kannan Ramchandran. Network coding for distributed storage systems. *IEEE Trans. Inf. Theory*, 56(9):4539–4551, 2010.

[42] Alexandros G Dimakis, Kannan Ramchandran, Yunnan Wu, and Changho Suh. A survey on network codes for distributed storage. *Proc. IEEE*, 99(3):476–489, 2011.

[43] Joan Daemen and Vincent Rijmen. *The Design of Rijndael: AES – the Advanced Encryption Standard*. Springer Science & Business Media, 2013.

[44] Costin Raiciu, Sebastien Barre, Christopher Pluntke, Adam Greenhalgh, Damon Wischik, and Mark Handley. Improving datacenter performance

and robustness with multipath TCP. *ACM SIGCOMM CCR*, 41(4):266–277, 2011.

[45] Swastik Kopparty, Srikanth V Krishnamurthy, Michalis Faloutsos, and Satish K Tripathi. Split TCP for mobile ad hoc networks. In *Proc. IEEE GLOBECOM*, volume 1, pages 138–142. IEEE, 2002.

[46] Elona Erez and Meir Feder. Efficient network code design for cyclic networks. *IEEE Trans. Inf. Theory*, 56(8):3862–3878, 2010.

[47] The Internet2 network.